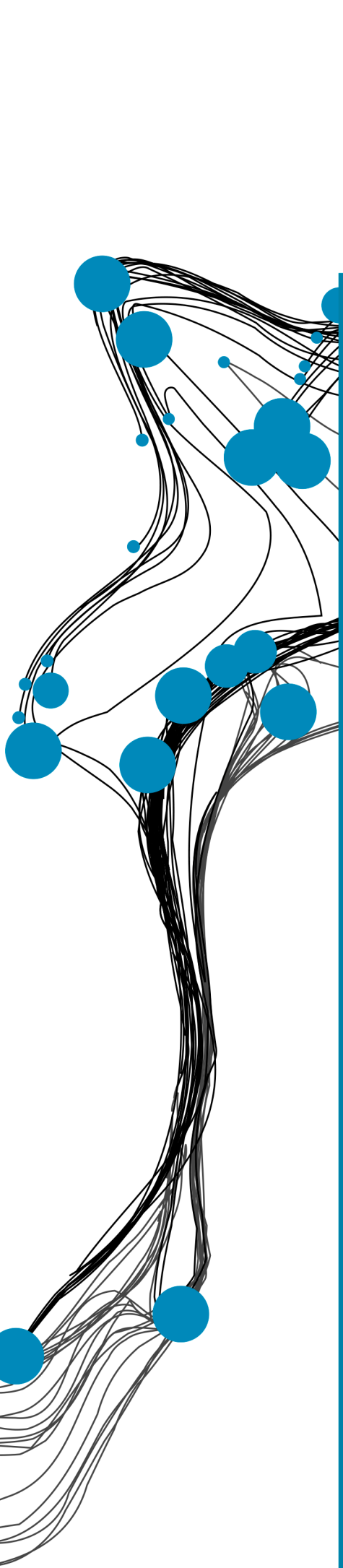

Influence and implementation of static balance on a parallel leaf spring mechanism

KOEN KLEVERWAL
M.Sc. THESIS MECHANICAL ENGINEERING
NOVEMBER 2023

University of Twente
Facutly of Engineering Technology

Project Supervisor: DR. IR. J.J. DE JONG ENGD
Academic Supervisor: PROF. DR. IR. D.M. BROUWER ENGD

Abstract

Flexure-based mechanisms have advantages over traditional mechanisms, as they do not suffer from backlash and friction, and have high precision and reliability. However, these mechanisms do have some drawbacks. The largest drawback is the strain energy storage in the flexible elements, which affects the input-output relationship, as a part of the inputted energy is used for the deformation of the elastic elements. To negate this effect, a system can be statically balanced. To do this, a compensating form of energy is introduced. This is often done by adding a pre-load in the mechanism. When in movement, energy can flow from the pre-load area to the deforming flexures. A system where the strain energy is compensated, in such a way that the potential energy is constant, is said to be statically balanced.

The addition of pre-load, leads to static balance, but also has effect on other system properties. The pre-load could affect the support stiffness of the mechanisms. Hysteresis could be added or increased, by the addition of pre-load. In this research, the side effects of pre-load are examined, with a focus on support stiffness, hysteresis and stress. Simulations and measurements were done, to examine the effects of the pre-load. Both modal measurements and hysteresis tests were done. The measurements were done with both mass and springs. The springs were both clamped and hanging. This was done so that the difference between attachment methods could be examined.

From the simulations it follows that the actuation stiffness, support stiffness and stress decrease when pre-load is applied. The actuation stiffness decreases linearly with increasing pre-load and can become negative. The support stiffness decreases with approximately 15% when one time the theoretical balancing load is applied. The stress decrease was found to be about 25 MPa at 1.5 to 2 two times the theoretical balancing load, for a leaf spring thickness of 0.4 mm. The stress decreases allows the leaf spring thickness to increase. An increase of leaf spring thickness of 0.1 mm leads to a stress increase of approximately 25 MPa and a support stiffness increase of about 25% when in equilibrium position. In deflected position, the increase is about 80%.

From the modal measurements, a decrease of 92.6% in eigen frequency in movement direction was found for the mass. For the spring, the largest decrease was found to 62.9%. No larger decrease could be acquired, as an increase in pre-load would lead to an unstable systems. The support eigen frequency drop by about 12% for the mass, and about 15% for the spring. This trend matches the simulations, therefore it can be concluded that the simulations are correct.

From the hysteresis measurements, it follows that the system with the mass becomes balanced at 11.75 kg. The system with the clamped spring becomes balanced at around 198 N, the system with the hanging spring becomes balanced at about 193 N. No large differences in hysteresis due to pre-load application method has been seen.

Contents

1 Introduction

Flexure-based mechanisms differ from traditional mechanisms, as they do not rely on movable joints for movement, but are able to move by elastic deformation [1]. This gives flexure-based mechanisms certain advantages over traditional mechanisms. These can be put into two categories: cost reduction and increased performance. The increase in performance comes from increased precision, increased reliability, and reduced wear. [1]. The precision of flexure-based mechanisms can be higher than traditional mechanisms, as flexure-based mechanisms do not suffer from backlash and are frictionless.
However, flexure-based mechanisms also have some drawbacks. One of those drawbacks is the strain energy storage in flexible elements [2]. This affects the input-output relationship of the mechanism [3]. Part of the inputted energy is not transferred to the output but is used for the deformation of the flexure-based elements. To negate this unwanted effect of energy storage, another form of compensating energy can be introduced. This can be done by applying a form of pre-load. Energy will flow from the pre-loaded area to the deforming area when the mechanism is displaced [4]. A system where the strain energy is compensated, in such a way that the potential energy is constant, is said to be statically balanced [5]. Gallego and Herder [3] derived five criteria for static balancing. These are constant potential energy, continuous equilibrium, neutral stability or zero stiffness, zero virtual work, and zero natural frequency.
A constant potential energy eliminates the actuation force and stiffness in the movement direction, resulting in zero natural frequency. Due to these advantages, statically balanced flexure-based mechanisms are used in multiple engineering fields, like medical devices such as grippers, and in precision machines [6].

There are multiple methods of implementing a pre-load. Often used methods are by adding mass or adding springs [5]. Adding mass is simple and accurate, but increases the mass of the system, which could be undesired. Springs also introduces a form of compensating energy. Multiple methods and different kinds of springs are possible for applying pre-load. A tension spring has been used by Merriam and Howell [7] and by Henein [8]. The first achieved an 87% reduction and the latter a 99.9 % reduction in actuation stiffness.
Rotational springs are used by Merriam et al. [9]. A large reduction was found in needed torque per displacement.
The geometry of a system can be designed in such a way that the geometry provides the compensating energy. This way it can directly be integrated into the system, as is done by Henein [8]. Liang et al. [10] used buckled leaf springs as a source of compensating energy. This design also results in a stiffness reduction in the driving reduction. Van Eijk and Dijksman use a plate spring with a negative stiffness [11].

Next to (partially) achieving static balance, pre-loading has an effect on other system properties and behavior. The support stiffness can decrease when a pre-load is applied [12]. This could be undesired and prove to be a problem in some situations. Adding external members to a system can increase hysteresis. This is the case for both the mass and the springs. Kim and Herder [13] found that their system suffers from a noticeable hysteresis loop and that it had a finite offset from zero force.

The stresses in the mechanism are affected by the pre-load. The maximum stress reduces when a leaf spring is put under pre-load [12]. When the pre-load is added, the stress is distributed more evenly over the leaf spring, such that the maximum stresses are reduced. This is only the case until a certain amount of pre-load. Due to this stress decrease, it becomes possible to increase the thickness of the leaf spring. A thicker leaf spring experiences higher stresses, but also results in a potentially higher support stiffness.

Most research conducted on flexure-based mechanisms is done on implementing pre-load and determining the quality of static balance. What is currently lacking, are the mentions of the side effects of static balancing, such as the effect on the support stiffness, the effect on the stress, and the hysteresis of the system. The decrease in support stiffness is mostly mentioned by analytical results and not derived or validated with experiments. The relation between stress decrease and potential support stiffness increase is also not mentioned. Hysteresis has been mentioned, but no relation has been made between the addition of pre-load and the hysteresis.

List of contributions In this research, the focus will be on the side effects of pre-loading. We investigate the effect of pre-load on the hysteresis, actuation stiffness, and support stiffness. This will be done with analytical models, FMB software, and measurements. The measurements which are done on the hysteresis of the system and the eigen frequencies. The difference between pre-load application method will also be examined.
An analytical model, the simulations, and measurements are discussed in Section 2. The results of the measurements can be seen in Section 3. In Section 4, the results, the effect of pre-load, the effect of pre-load application method, and the relation between stress decrease and stiffness increase are discussed. The conclusion can be seen in Section 5.

2 Method

2.1 Pre-load to achieve static balance

Pre-load has to be applied to static balance the system. Multiple methods of applying pre-load are possible. The amount of pre-load to achieve balance has to be determined. With the balancing load determined, an analytical model can be made and examined. From there on the methods of applying pre-load in a setup will be discussed. The effects of the pre-load will be analyzed with the help of simulations. With the analytical model and the simulations, a design setup will be made. This setup will be analyzed, to examine the effects of pre-load. To do this, a measurement plan will be made.

2.1.1 Buckling load and form

The theoretical balancing load is based on the buckling load. This can be determined with Equation 1. This formula represents the amount of force that is needed to achieve buckling in a leaf spring. The value K corresponds with different buckling modes [14]. In this case of value 1 is the relevant value for K.

$$P_{cr} = \frac{1}{K^2}\frac{\pi^2 EI}{L^2} = \frac{\pi^2 EI}{L^2} \tag{1}$$

Wherein E is the E-modulus of the material, L is the length of the leaf spring and I is as follows:

$$I = \frac{1}{12}wt^3$$

Where w is the width of the leaf spring and t is the thickness of the leaf spring. With the theoretical amount of pre-load to balance a system known, an analytical model can be made to analyze the effect of the pre-load.

2.1.2 System properties

In Figure 1, a drawing of a parallel leaf spring mechanism and a leaf spring can be seen. The variable names for certain system properties can be seen. The properties of the leaf spring can be seen in Table 1.

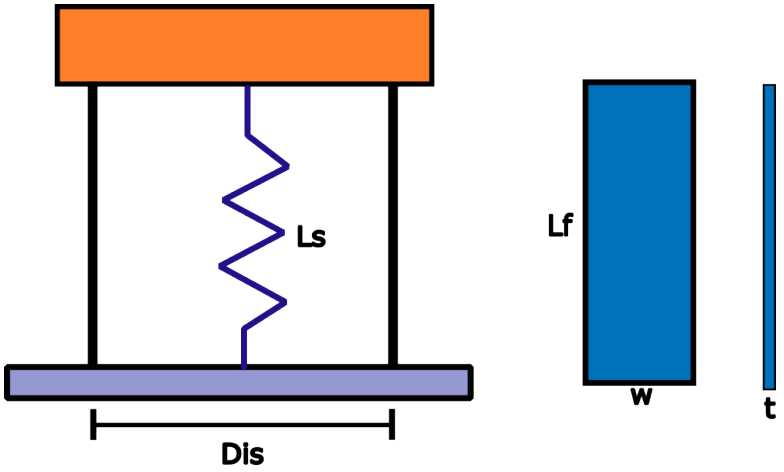

Figure 1: Model of the parallel leaf spring mechanism, and a leaf spring

Table 1: Leaf spring properties

Property	Variable	Value
Length	L_f	94 mm
Width	w	54 mm
Thickness	t	0.4 mm
Distance	Dis	78 mm

The basic system properties can be found using analytical formulas. In Equation 2 and Equation 3, the formula for the actuation stiffness and the support stiffness can be seen.

$$k_x = \frac{Ewt^3}{L^3} \tag{2}$$

$$k_y = \frac{EA}{L} = \frac{Ewt}{L} \tag{3}$$

The stress of the mechanism can also be calculated. The bending stress can be found with Equation 4. The compressive stress can be found with Equation 5.

$$\sigma_b = -\frac{My}{I} \tag{4}$$

$$\sigma = \frac{F}{A} \tag{5}$$

2.2 Rigid arm equivalent and analytical model and of vertical force

A parallel leaf spring mechanism experiences shortening when displaced from the equilibrium position. The movement of the mechanism represents a circle movement. This behavior can be seen in Figure 2. This movement can also be modeled as a rigid arm. The rigid arm is fixed at one end and rotates in the same fashion as the parallel leaf spring mechanism does.

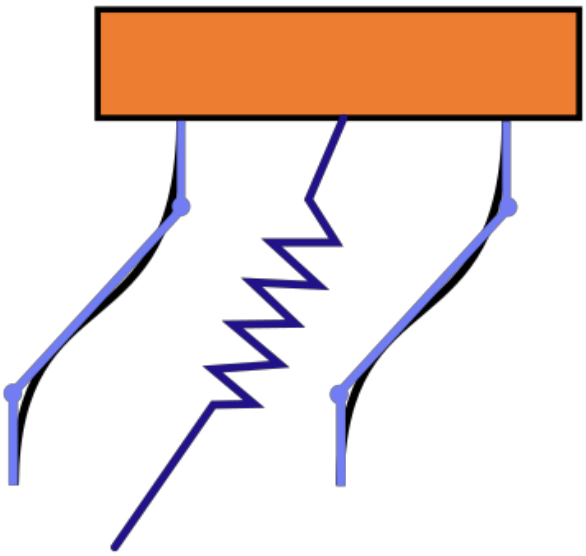

Figure 2: Deflected parallel leaf spring mechanism

Basic model of rigid arm equivalent

The basic model consists of a rigid arm, attached at the bottom, making it such that the arm can rotate freely, and a horizontal spring. This spring simulates the stiffness in the driving direction. Multiple lengths are present in the analytical model. The length of the flexure is named L_f. The length of the rigid arm is denoted as L_r, and is modeled with a length of $\frac{5}{6}L_f$. This is due to the way the flexure deforms when displaced, as can be seen in Figure 2 and Figure 3.

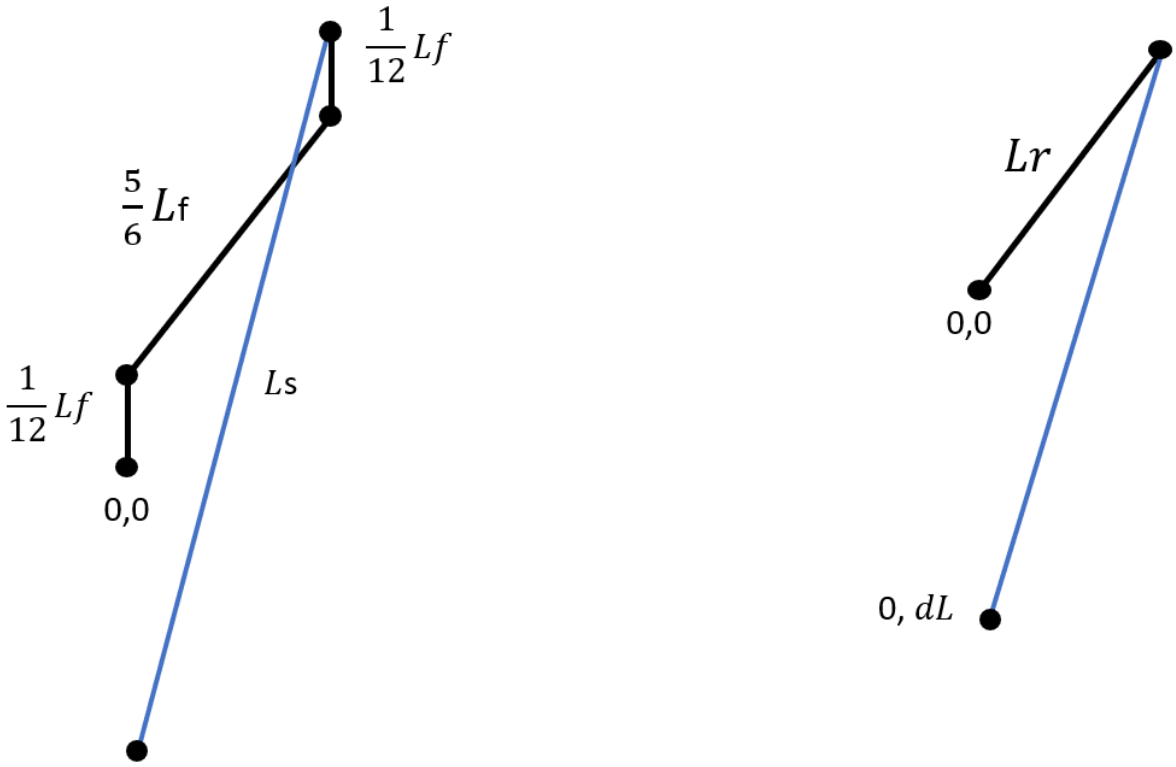

Figure 3: Model of the rigid arm.

From this, a free body diagram (FBD) can be made. This free body diagram can be seen Figure 4. Two forces and a spring can be seen. F_x is used to displace the rigid arm. F_y is used to simulate the pre-load of the system and the mass of the system. The spring has a spring stiffness equal to the actuation stiffness. This actuation stiffness can be found with Equation 2. In the equation, the actuation stiffness is found for one leaf spring, so the found value has to be multiplied by a factor of two. This found stiffness will be denoted as k_x. The amount of force this horizontal spring gives is dependent on the displacement of the rigid arm, this displacement is denoted with dx. The spring force is denoted as F_f.

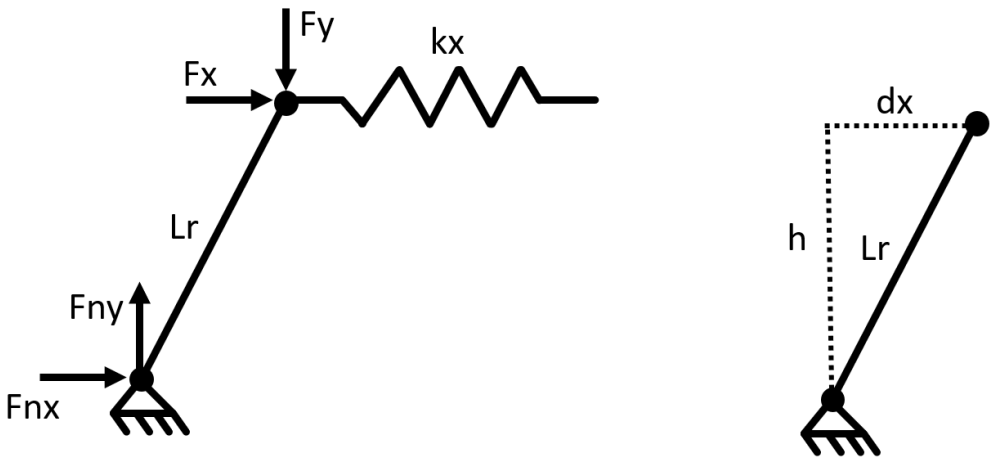

Figure 4: FBD of the rigid arm

The length of the rigid arm can be divided into its components in the x- and y- direction. The x-direction is known, which is equal to the displacement dx. The y-direction can be found using Pythagoras' Theorem and can be seen in Equation 6.

$$h = \sqrt{L_r^2 - dx^2} \tag{6}$$

With the free body diagram and the lengths known, the force and moment balances can be found. These can be seen below.

$$\Sigma F_x = F_x + F_{n,x} - F_f = F_x + F_{n,x} - k_x dx \tag{7}$$

$$\Sigma F_y = -F_y + F_{n,y} \tag{8}$$

$$\Sigma M = -F_x h + F_f h - F_y dx \tag{9}$$

With the force and moment balances found, the unknowns in these equations can be found.

$$F_{n,y} = F_y \tag{10}$$

$$F_x = F_f - F_y \frac{dx}{h} = k_x dx - F_y \frac{dx}{\sqrt{L_r^2 - dx^2}} \tag{11}$$

$$F_{n,x} = F_f - F_x \tag{12}$$

With the forces and system properties known, the effect of the pre-load on actuation stiffness can be found. This can be seen in Figure 5. Here the actuation stiffness is evaluated for an increasing pre-load.

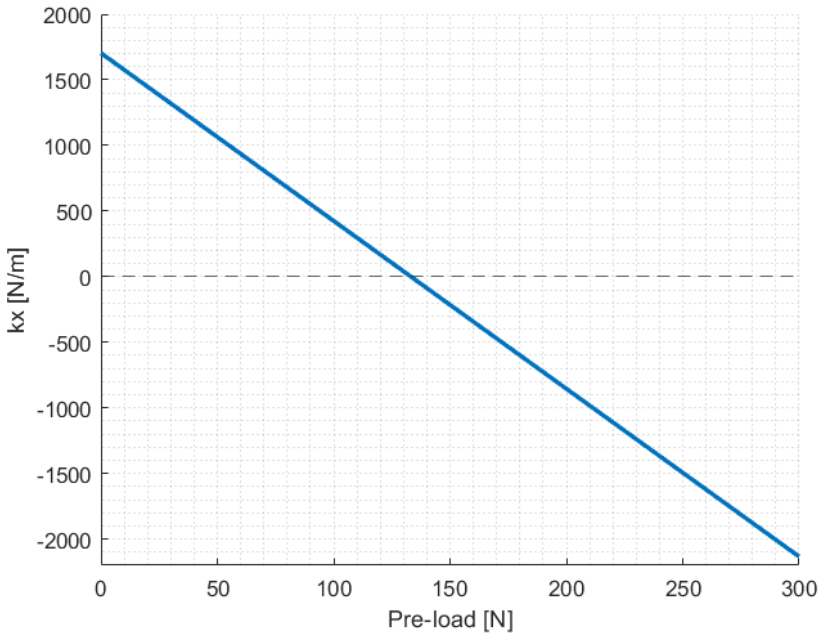

Figure 5: Actuation stiffness over pre-load

It can be seen that after a certain value of pre-load, the stiffness becomes negative. From that point, the system becomes statically balanced. The relation between the stiffness decrease and pre-load is linear.

2.3 Applying pre-load

In the analytical model seen above, the pre-load was applied as a vertical force. Such a theoretical force cannot be inputted in a real-life setup. So other methods of adding pre-load need to be used, the forms used are adding a mass and adding a spring.

2.3.1 Mass

Mass can be used to balance a system. Mass brings the disadvantage that the total mass of the system increases. The force of the mass is always in the direction of the gravity. This could be an advantage and a disadvantage. If the parallel leaf spring mechanism is situated correctly, the force acts perpendicular to the movement direction, which is in this case desired.

2.3.2 Springs

Another method of adding pre-load is by adding a spring. In this research tension springs will be used. A tension spring has a starting length, this starting length is said to be a zero length and is denoted as L_0. At the zero length, the spring has a force that is present, this force is called the zero force and is denoted by F_0. The spring will not move if it is excited with a force smaller than the zero force of the spring. When an applied force is larger than the zero force, the spring will move. The behavior of the spring from that point on is linear, where a displacement from the applied force is determined by the spring constant. The spring constant is denoted by k_s. It is not possible to add a standard tension spring with a pre-load value of zero.
The spring force acts in line with the spring. This is not always perpendicular to the movement direction, as the spring moves over the same circle as the parallel leaf spring mechanism does, due to the shortening of the leaf spring mechanism. When the mechanism is deflected, this results in a spring force component perpendicular to the movement direction, and a component opposite of movement direction.
A spring has its own dynamic effects. When a spring is added to the mechanism, these dynamic effects also have an influence on the behavior of the mechanism. It is possible that a spring adds hysteresis to a system, or increases the present hysteresis in the system. Friction and play in the attachment can increase the hysteresis of the system.

2.3.3 Increasing the pre-load

To get a good overview of the effects of pre-load, the pre-load can be added in steps and increased to the final value. The pre-load is increased by either adding mass or increasing the length of the spring. The mass and spring are used independently. The needed length of the spring is calculated by dividing the found theoretical balancing load by the spring stiffness.

2.3.4 Effects of pre-load on system properties

Stiffness and stress
As mentioned before, the applied pre-load has desired and undesired effects. The desired effect is that the driving stiffness and the corresponding eigen frequency decrease to (close to) zero. The support stiffness could drop when pre-load is applied, this could be undesired.
A positive effect of pre-load is the maximum stress decrease in the leaf springs. In itself, this is a desired effect, but another advantage of the maximum stress decrease is to possibility of increasing the thickness of the leaf springs, which in turn increases the support stiffness. As can be seen in Equation 3, larger thickness results in a higher value for k_y. When the thickness is increased, the stiffness in the movement direction is also increased. This can be seen in Equation 2. The leaf spring thickness has an influence on the driving stiffness with a power three. The increase could be undesired. A larger thickness can result in a higher bending stress, due to the fact that the internal moment increases. The compressive stress decreases as the area decreases with increasing stiffness, as can be seen in Equation 5. It is also known that the maximum stress decreases when pre-load is applied, this is due to a more even stress distribution over the leaf spring. This results in there being an optimal value of pre-load and leaf spring thickness for driving stiffness, support stiffness, and stress.

Hysteresis
Adding extra components to a system can increase the hysteresis in a system. The hysteresis could come from the attachment of the spring or the attachment of the mass. The pre-load could also increase the already present hysteresis in the system. A higher hysteresis results in decreased repeatability, which is undesired.

2.4 Analytical model of mass and spring

The analytical model seen before can also be used to analyze the cases where pre-load is added with the mass or with the springs.

2.4.1 Mass

The analytical model of the mass is the same as the analytical, which can be seen in Figure 4. The pre-load in kilograms can be converted to Newtons and can be added to the system. From this, the effect of pre-load on stiffness can be analyzed. This can be seen in Figure 6.

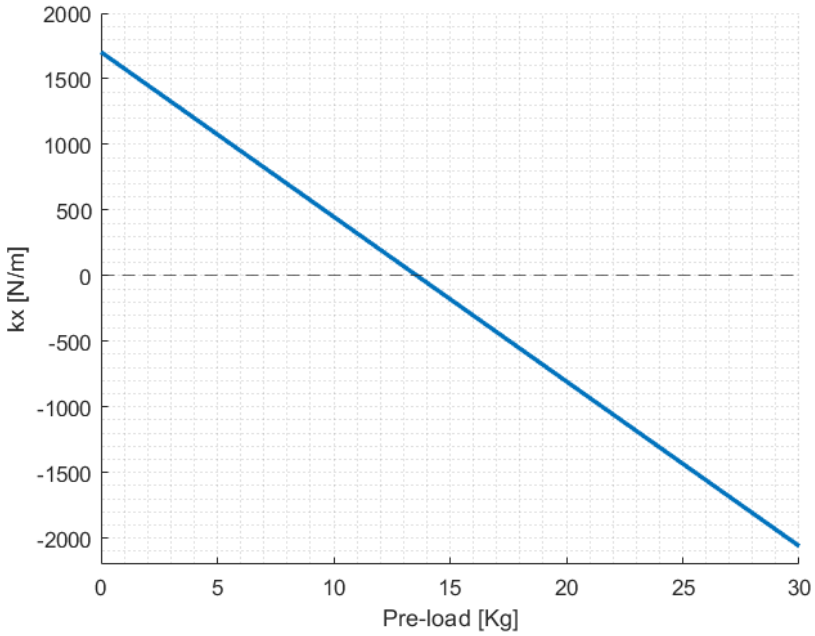

Figure 6: Stiffness over pre-load, for the mass case

It can be seen that the stiffness decreases with an increasing pre-load. At a pre-load of about 13.5 kg, the stiffness becomes negative.

2.4.2 Spring

The analytical model used before is not representative of the system with the spring. The spring adds pre-load to the system needs to be added. This spring is attached at the top of the rigid arm. dL is the distance from the attachment bottom attachment point to bottom of the rigid arm, as can be seen in Figure 3. The length of the spring is denoted by L_s. The length of the spring can be derived with Equation 13. With the spring length and stiffness known, the spring force can be found. This can be done with Equation 14.

$$L_s = \sqrt{(dx^2 + (h + dL)^2)} \tag{13}$$

$$F_s = k_s(L_s - L_0) + F_0 \tag{14}$$

A free body diagram is made and can be seen in Figure 7. F_y is still present, this is done to simulate the mass of the mechanism.

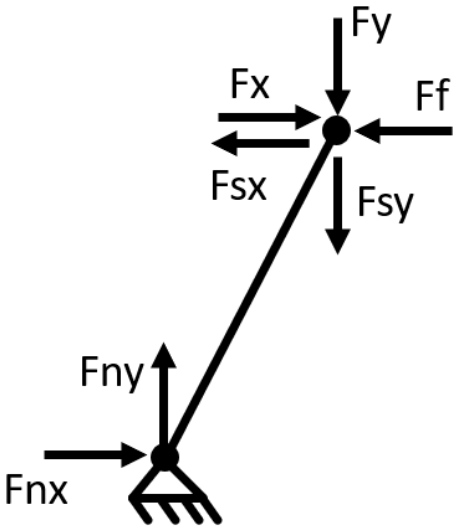

Figure 7: FBD of the analytical model with spring

The spring force can be divided into components in x- and y-direction. This is done with Pythagoras' theorem. A factor r is derived, which gives the ratio between the lengths in the x- and y-direction. This factor r can be seen in Equation 15. Using this factor, the spring force in the y-direction can be found with Equation 16. The force in x-direction can then be found with Equation 17.

$$r = \frac{dx}{(h + dL)} \tag{15}$$

$$F_{s,y} = \sqrt{\frac{F_s^2}{r^2 + 1}} \tag{16}$$

$$F_{s,x} = rF_{s,y} \tag{17}$$

From the free body diagram, the force and moment balances can be derived. These can be seen below.

$$\Sigma F_x = F_x - F_f - F_{s,x} - F_{n,x} \tag{18}$$

$$\Sigma F_y = -F_y - F_{s,y} + F_{n,y} \tag{19}$$

$$\Sigma M = F_f h - F_x h - F_y dx - F_{s,y} dx + F_{s,x} h \tag{20}$$

With the spring force known and the force and moment balances known, the following can be derived.

$$F_{n,y} = F_y + F_{s,y} \tag{21}$$

$$F_x = F_f - F_y \frac{dx}{h} - F_{s,y} \frac{dx}{h} + F_{s,x} \tag{22}$$

$$F_{n,x} = -F_x + F_f + F_{s,x} \tag{23}$$

From this, the effect of pre-load on the stiffness can be analyzed. This can be seen in Figure 8. This is evaluated for an increasing value of spring force, with a constant value for dL. This attachment point is placed at the arbitrary point of -100 mm from the bottom of the rigid arm. The spring properties are derived from a spring which will later on be used for the experiments.

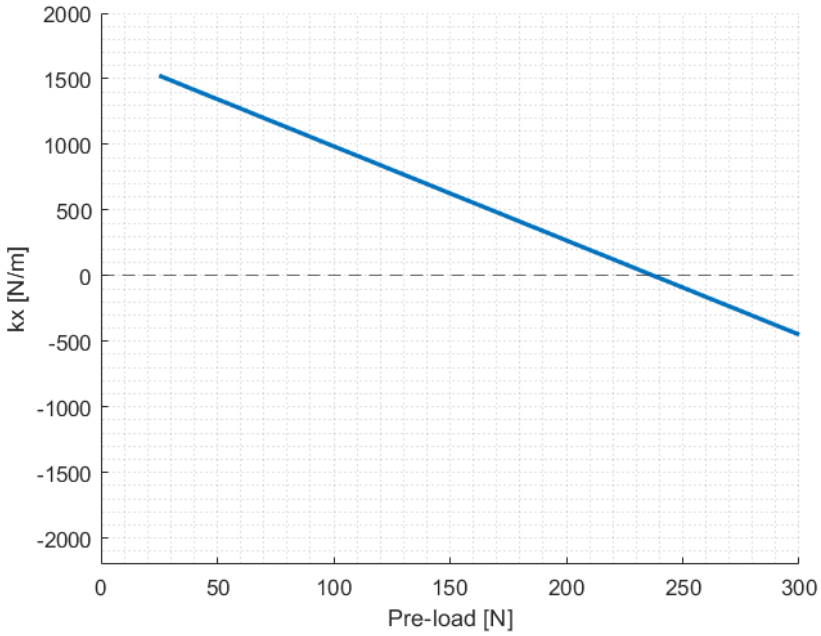

Figure 8: Stiffness over pre-load, for the spring case

It can be seen that a higher value of pre-load is needed to reach the point of zero stiffness. This is due to the stiffening effect of the spring, which will be explained below. Also, the zero force of the spring is taken into account, as no lower amount of pre-load can be used.

2.5 Effect of springs

It can be seen in Figure 5, Figure 6 and Figure 8 that the force needed to balance is higher for the case where a spring is added. This is due to the spring force having a component that is opposite of the movement direction. The force needed to reach a certain displacement increases, when compared with the case of the added mass of force. This effect can be seen as a stiffening effect by the spring, which is examined below.

2.5.1 Spring stiffening effect from analytical model

The stiffening effect of the spring can be seen in the force balances. When compared with the force and the mass, extra components can be seen in ΣF_x. These extra terms can be seen in Equation 24.

$$-F_{s,y}\frac{dx}{h} + F_{s,x} = -F_{s,y}\frac{dx}{\sqrt{L_r^2 - dx^2}} + F_{s,x} \tag{24}$$

It can be seen that a factor is present in front of the y-component of the spring force. This causes the x-component to have a larger influence. The x-component of the spring force is dependent on multiple factors, which are:

- Spring constant k_s
- F_0
- Spring length L_s
  - Attachment point bottom dL
  - L_0
- Deflection dx

The force is dependent on the spring stiffness and the location of the attachment points of the spring. With that, the following can be derived:

$$F_{s,x} = rF_{s,y} = \frac{dx}{h + dL}F_{s,y} \tag{25}$$

$$\frac{dx}{h + dL}\sqrt{\frac{F_s^2}{(\frac{dx}{h+dL})^2 + 1}} = \frac{dx}{h + dL}\sqrt{\frac{1}{(\frac{dx}{h+dL})^2 + 1}}F_s \tag{26}$$

$$\frac{dx}{h + dL}\sqrt{\frac{(k_s(L_s - L_0) + F_0)^2}{(\frac{dx}{h+dL})^2 + 1}} \tag{27}$$

$$\frac{dx}{h + dL}\sqrt{\frac{(k_s(\sqrt{dx^2 + (h + dL)^2} - L_0) + F_0)^2}{(\frac{dx}{h+dL})^2 + 1}} \tag{28}$$

$$\frac{dx}{\sqrt{L_r^2 - dx^2} + dL}\sqrt{\frac{(k_s(\sqrt{dx^2 + (\sqrt{L_r^2 - dx^2} + dL)^2} - L_0) + F_0)^2}{(\frac{dx}{\sqrt{L_r^2 - dx^2}+dL})^2 + 1}} \tag{29}$$

Some variables in Equation 29 are dependent on the chosen spring and cannot be changed. What can be changed is the amount of displacement dx and the attachment point of the spring dL. A decrease in dx results in a lower value of the spring force in x-direction. As does an increase in dL, however, an increasing dL also results in a higher spring force.

2.5.2 Spring stiffening effect quantified

The stiffening effect can be quantified and is in proportion to the theoretical buckling load, the length of the spring, and the length of the leaf springs. With Equation 30, this effect can be calculated.

$$F_s \approxeq \frac{12L_s}{12L_s - \pi^2 L_f}F_{balance}[12] \tag{30}$$

Wherein $F_{balance}$ has previously been seen as P_{cr} in Equation 1.

In Figure 9, the normalized force can be seen over the normalized length of the spring can be seen. The force is normalized to the theoretical balancing force, for a leaf spring of 0.4 mm thick. The length is normalized to the length of the leaf spring. The largest effect can be seen in the range of the length of the leaf spring. The stiffening effect is very large when the spring has the same length as the flexure. From a spring length of 1.5 times the flexure length, the effect is manageable. The behavior becomes asymptotic when the length is increased and the needed force gets really close to the theoretical balancing force.
It can be seen that the needed balancing force is lower than the theoretical buckling force when the spring has a negative length. A negative length corresponds with a compression spring.
It can be seen that at a length of 0 and a pre-load of 0, the system should be balanced, this can not exist in a mechanism. A length of 0.1 would result in a small negative pre-load, this could also not be the case. It therefore is assumed that this formula cannot give a good indication of needed pre-load at and around a length of 0.

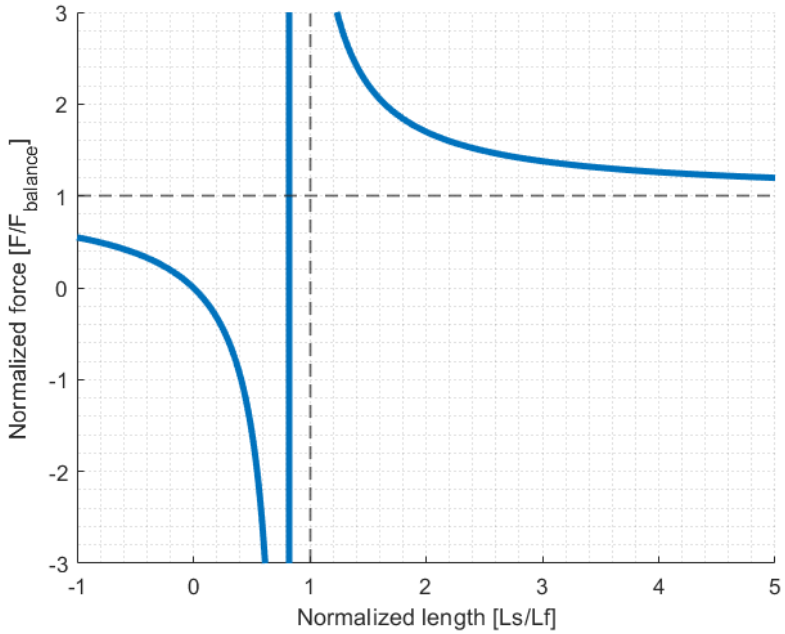

Figure 9: Stiffening effect as follows from Eq. 30

2.5.3 Effect of spring length

The spring force has a component acting in the opposite direction of the movement direction. When the mechanism is deflected, the spring is put under an angle. A larger angle results in a larger component of the spring force in the opposite direction of the movement direction. The angle decreases for a larger spring when compared with a shorter spring. A larger spring thus reduces the stiffening effect. This can also be seen in Equation 29, an increase in dL results in a lower value of the spring force opposite of movement direction.
This influence of spring length can also be seen in the stiffness of the mechanism, as can be seen in Figure 10. A lower pre-load results in a lower stiffness, as expected. It can also be seen that for the same amount of pre-load, a longer spring results in a lower stiffness, as is expected.

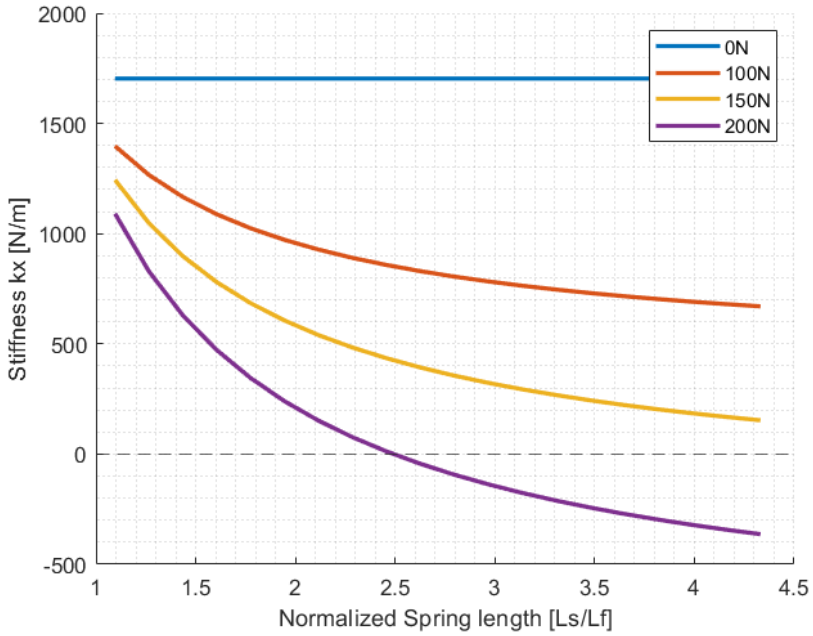

Figure 10: Stiffness in the movement direction, with changing spring length

2.6 Simulations

Multiple simulations were done in the modeling software SPACAR [15]. The simulations were done with a model consisting of two vertical leaf springs and a connection part. These leaf spring consists of multiple flexible parts. The leaf springs are connected to each other using a rigid body at one end and are fixed at the other end. For the relevant simulations, a truss is added to simulate a spring. Mass is added to simulate the mass of the setup itself. Mass is also used to add pre-load, for the case where mass is added to the system.
The eigen frequencies of the system can be evaluated in SPACAR. The first ten eigen frequencies are given. The corresponding eigen modes can be displayed. The stress in the system can be calculated in SPACAR, and the stress distribution can be displayed. The compliance of the leaf springs can be calculated. With the compliance, the stiffness can be found. The simulations can be evaluated in both the equilibrium position and over deflected positions.

2.7 Design setup

The design is based on a parallel leaf spring mechanism. Two leaf springs are mounted at a bottom plate and a top plate using clamps. The leaf spring mechanism is placed on beams, which are attached to the bottom of the leaf spring mechanism and on another plate. This plate has rubber supports on the bottom. The top plate has an attachment point for a spring. The bottom plate of the leaf spring mechanism has a hole, to allow the spring to pass through. This is done so that a spring can be longer than the leaf springs. A spring can be attached to the top plate. The other end of the spring can be attached to a mechanism that can move up and down over a guide and a spindle. The length of the spring can be decreased or increased by moving the spindle. End stops in movement direction are added to make sure that the mechanism does not move too far to either side.
The SolidWorks model can be seen in Figure 11a. The build model can be seen in Figure 11b. To apply an external force to the system, a voice coil motor (VCM) [16] is attached to one side of the mechanism. The VCM line of action passes through the center of compliance. An encoder [17] is placed at the same height.
The springs can be attached in two ways. It can be hanging on screws, which are placed on the attachment points, or it can be clamped to the attachment points. The hanging on a screw design can be seen in Figure 12a. The clamped situation can be seen in Figure 12b. The attachment point at the spindle uses the same methods of attaching.

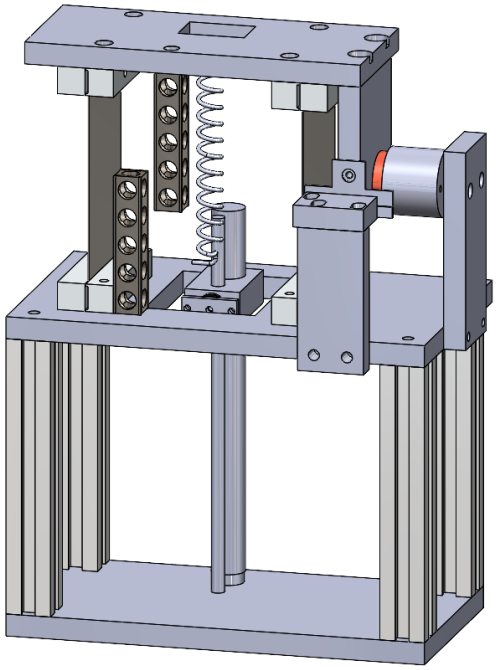

(a) Solidworks model of the setup

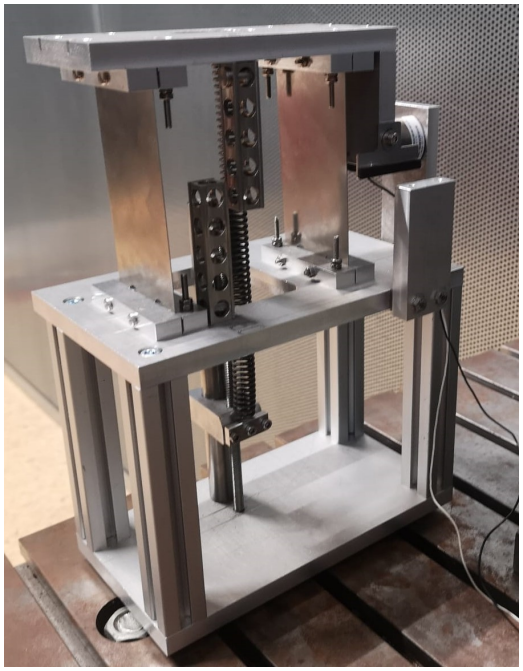

(b) Picture of the setup, without encoder

Figure 11: Solidworks design and build setup

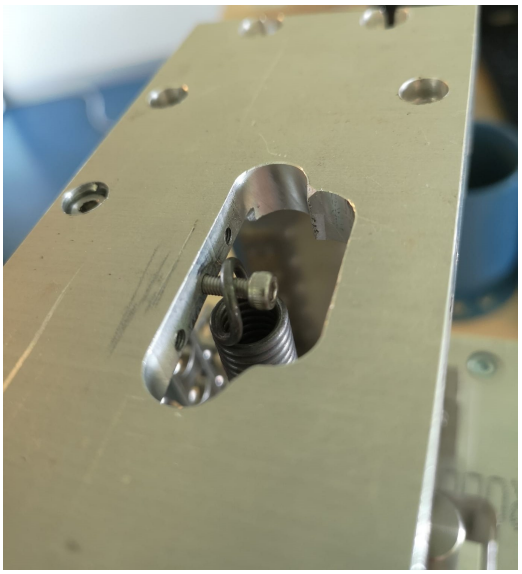

(a) Hanging spring setup

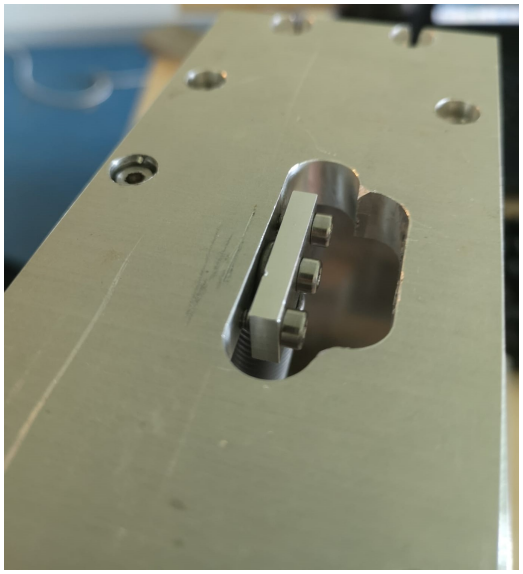

(b) Clamped spring setup

Figure 12: Setups of spring attachment

2.8 Measurement plan

Multiple measurements will be done, to gather data on the behavior of the system and to validate the simulations. Two types of tests will be done, modal analysis and hysteresis tests. The modal analysis can tell about the effect of pre-load on the driving eigen frequency and the support eigen frequency of the system. These measurements can also be used to validate the simulations. The hysteresis test can tell about the hysteresis in the system, the hysteresis the spring possibly adds, and the hysteresis of the system where mass is added. The hysteresis tests can also be used to find the balance point of the system. The tests will be done with both mass added and springs added.

2.8.1 Springs used

Three springs are acquired to use for the tests. Multiple springs are used such that the spring length and amount of pre-load can be changed semi-independently. The name used in the report, the manufacturer-specified name, the zero-length of each spring the manufacturer-specified stiffness, and the measured stiffness can be seen in Table 2. The spring stiffnesses are identified and can be seen in Appendix A. In the report the results of spring B are shown, this spring is mentioned with the word spring. The results for Spring A and C can be seen in the Appendix. The springs are ordered from TEVEMA [18].

Table 2: Classification of the springs

Report name	Manufacturer name	L_0 [mm]	F_0 [N]	Specified stiffness [N/mm]	Measured stiffness [N/mm]
A	T32074	75.8	23.3	3.33	3.423
B	T32235	123	24.38	1.71	1.750
C	T32681	128	85.9	11.34	12.3

To determine the pre-load of the springs, the amount of turnings of the spindles is counted. With the pitch of the spindle and the stiffness, the exact amount of pre-load can be determined. The starting position of the spring is determined by moving the spring up to the top plate. When the spring cannot move further up and deflects to the side, the spring is moved down with one turn of the spindle. The position the spring is in at that point is chosen to be the starting position.

2.8.2 Hysteresis test setup

The hysteresis test is done with the VCM and encoder present on the system. The input to the VCM is a sine wave. The input force is not measured. It is assumed that the force is proportional to the input current when the VCM is moving slowly [19]. The force can be found with the motor constant and the inputted current. The motor constant can be identified by examining the change of bode plots with different pre-loads.
The system is position-controlled with a PID controller. The initial tuning is done with the tuning rules of the lecture notes of Aarts and van Dijk [20]. The mass equivalent needed has been found by running an identification, and can be seen in Figure 31.

2.8.3 Modal Analysis setup

The quality of static balance can be analyzed by a modal analysis. The eigen frequency can tell about the amount of balance of the mechanism. When the eigen frequency is zero, the system is balanced.
The modal analysis will be done with a laser-vibrometer, in this case, the Polytec PSV-500 [21] is used. The laser-vibrometer is positioned perpendicular to the leaf spring and shines a laser at a spot on the leaf spring. The machine measures the movement of the spot. This is done for multiple points. After every spot is measured, a model of the mode shapes and the eigenfrequencies is made. In these tests, 25 evenly dived points are measured. The mechanism was exited by a sweep. The settings of the laser-vibrometer can be seen in Table 3.

Table 3: Settings used in the laser-vibrometer

Setting	**Value**
FFT Lines	3200
FFT magnitude averaging	off
Amplitude	2
Voltage	[-2,2]
Sweep time	3.2 sec
Sweep range	1-1000 Hz
Measuring range	125 mm/s
Measuring bandwidth	0-1000 Hz
Resolution	312.5 mHz

3 Results

3.1 Force-displacement plots

3.1.1 Analytical and simulated force-displacement plots

In Figure 13a and Figure 13b, the force displacement plots of the mass and the spring can be seen. In a dotted line, the analytical results for the corresponding pre-loads are overlayed. It can be seen that the simulations and the analytical model match quite well. The same effect of increasing pre-load can be seen. The same amount of force is needed to reach the same amount of displacement.
An increase in force leads to an increase in displacement. From a certain amount of pre-load, the force needs to decrease to increase the displacement. The stiffness of the mechanism becomes negative.
It can be seen that a higher pre-load is needed to balance the spring case. This is expected from the analytical model.

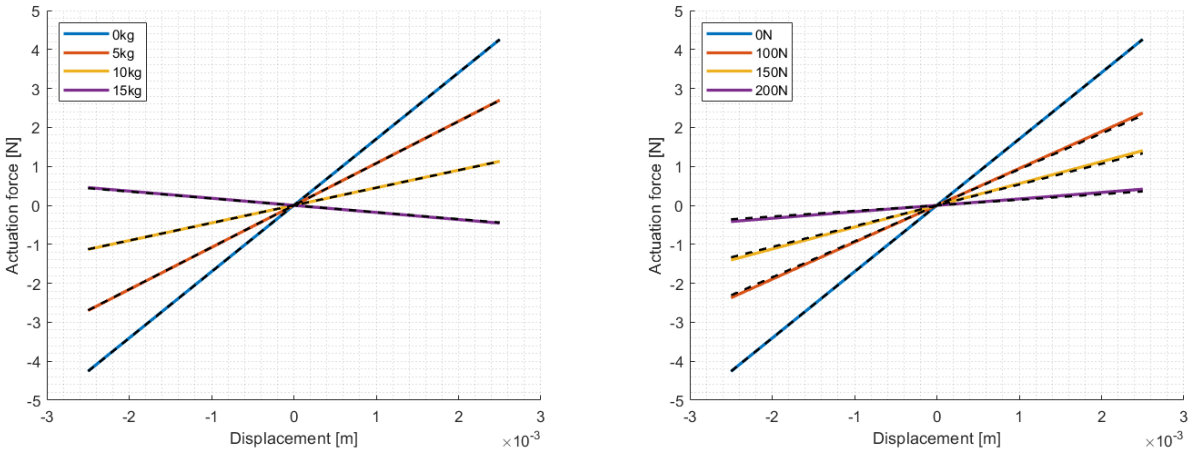

(a) Force displacement plot of the mass

(b) Force displacement plot of the spring

Figure 13: Analytical and simulated force displacements plots of the mass and spring

3.1.2 Measured force-displacement plots

The simulated and analytical force displacement plots can be compared with measurement results. The force is not measured in the tests, but the effect of pre-load can be compared. The force can also be estimated with the motor constant. The motor constant was estimated to be $3.23N/A$. This value was used to determine the actuation force.
In Figure 14, the results for the hysteresis test of the mass can be seen. In Figure 15, the hysteresis curves of the clamped spring can be seen. In Figure 16, the hysteresis curves of the hanging spring can be seen. The figures are divided into the range of pre-load, and the values close to balancing force.
From the measurements, it can be seen that a higher pre-load results in a less steep line. Less force is needed to get the same displacement, meaning that the stiffness drops. At a certain pre-load, the system becomes (close to being) balanced, the curves lay flat. This is due to the force needed to displace the mechanism is close to zero. Beyond the balancing point, the curves tip over. In that case, there is negative stiffness present. The force needs to decrease to increase the displacement.
It can be seen that in the case of the springs, more pre-load is needed to achieve the same effect in the case of the mass. This is expected, as this is derived from the analytical model. Approximately the same displacement is reached with the same force for both the mass and the springs. No significant difference is seen between the attachment methods of the springs.

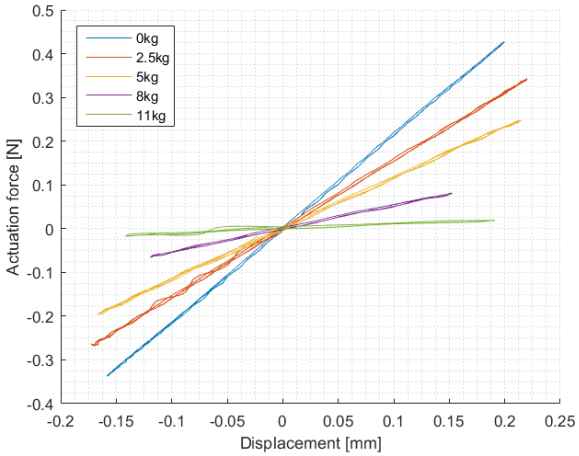

(a) Hysteresis plot of the mass

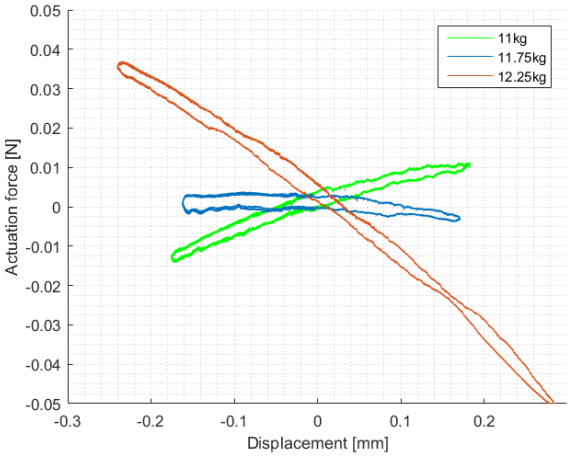

(b) Hysteresis plot of the mass, zoomed in

Figure 14: Hysteresis measurements of the mass

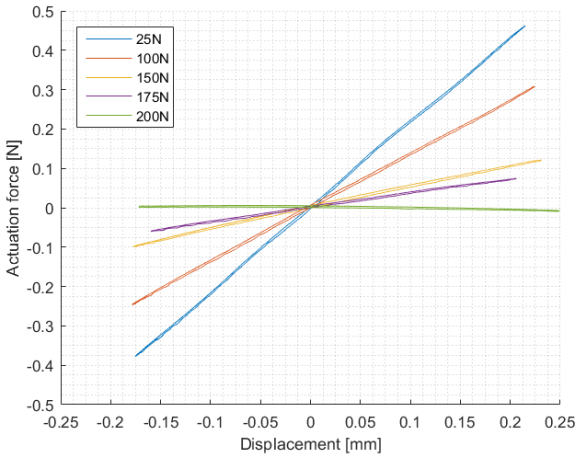

(a) Hysteresis plot of the clamped spring

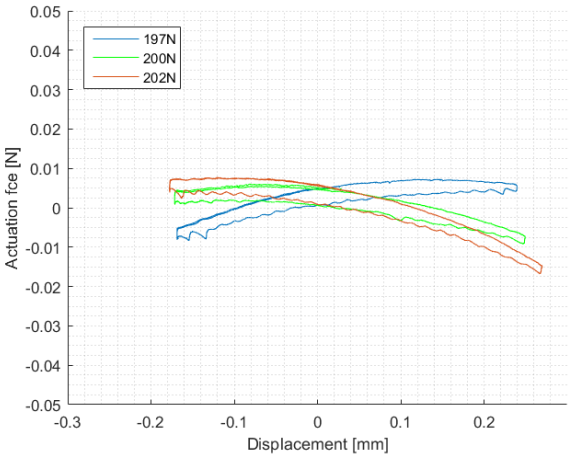

(b) Hysteresis plot of the clamped spring, zoomed in

Figure 15: Hysteresis measurements of the clamped spring

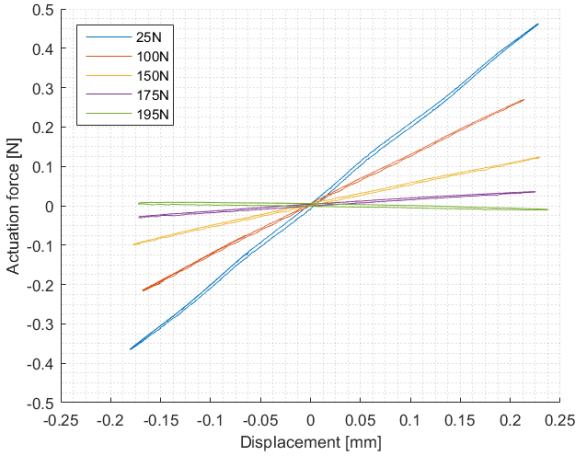

(a) Hysteresis plot of the hanging spring

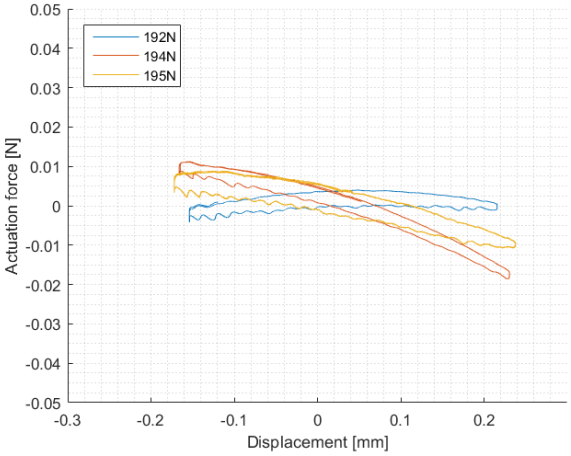

(b) Hysteresis plot of the hanging spring, zoomed in

Figure 16: Hysteresis measurements of the hanging spring

Quantified hysteresis

The hysteresis can be quantified around the equilibrium position, thus around a displacement of zero and at a force of zero. The percentage of hysteresis can be found from the mechanism with the lowest amount of pre-load. The quantified hysteresis is plotted over normalized pre-load. The pre-load is normalized to the theoretical balancing load of the leaf springs with a thickness of 0.4mm. The plotted hysteresis can be seen in Figure 17.

It can be seen that the force hysteresis is quite constant when the pre-load increases. The displacement hysteresis increases for a higher pre-load. When the system is (close to being) balanced, the displacement almost becomes equal to the whole displacement of the system. This is because the hysteresis curve is lying flat, almost no force is needed to move the mechanism. When the stiffness becomes negative, the hysteresis curve begins to slope down.

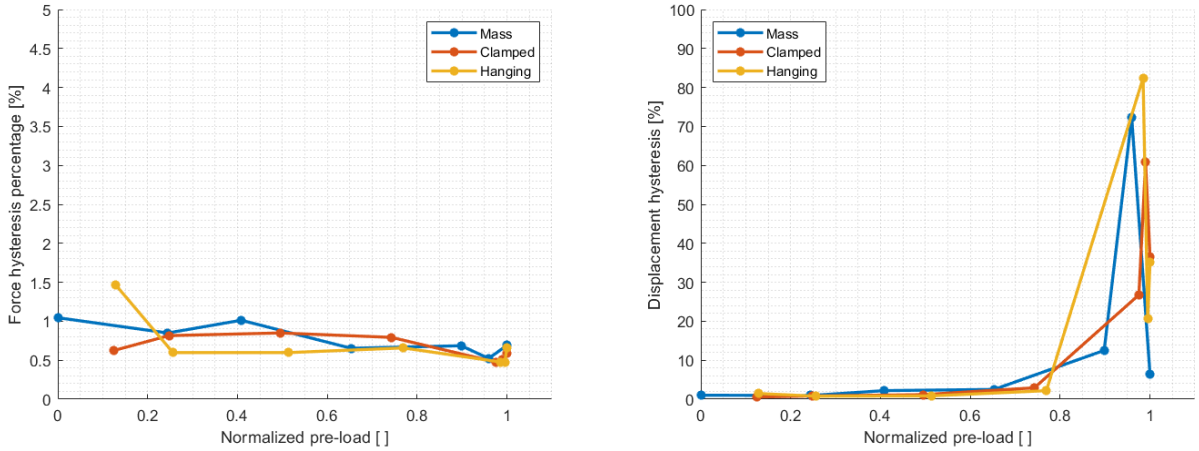

(a) Current hysteresis plotted over normalized pre-load (b) Displacement hysteresis plotted over normalized pre-load

Figure 17: Percentage of maximum force- and displacement hysteresis

3.1.3 Comparison with simulations

In Figure 18, the measured force displacement of the mass and spring can be seen with the simulated force displacement.

A smaller displacement is reached in the measurements when compared with the simulations. This is due to limitations in the current which is sent to the VCM. Still, the effect of the pre-load can be compared with the simulations. This is because the steepness of the force-displacement lines can be compared.

Approximately the same effect of pre-load can be seen in the simulated force-displacement plots and the measured force-displacement plots. The pre-load to achieve balance is lower in the measurements than it is in the theoretical results. This could mean that there are unmodelled compliances in the system. It can also indicate that the determined value of the motor constant is off.

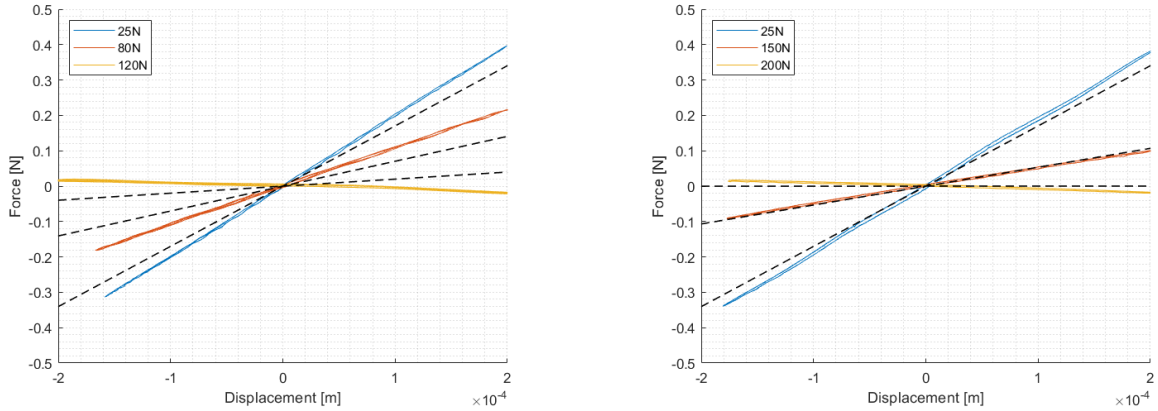

(a) Measured mass hysteresis compared with simulations (b) Measured spring hysteresis compared with simulations

Figure 18: Measured hysteresis compared with simulations

3.2 Simulated system properties

Simulations are used to give information on system properties and how the systems behaves in multiple situations. This can be an increase in pre-load, a displacement of the system, or an increase in leaf spring thickness. Below the simulated system properties can be seen.

3.2.1 Stiffness

Simulations were done in which the stiffness of the leaf springs was derived. The stiffnesses are divided into the driving stiffness and the stiffness of the leaf spring in the support direction.
The stiffnesses are examined for different leaf spring thicknesses and different values of pre-load. These are examined in equilibrium position, deflected position, and over a range of movements.

Driving stiffness
The results for the stiffness in the driving direction can be seen below. In Figure 19, the stiffness for both the mass and spring can be seen, where the pre-load is normalized to the theoretical balancing load for the corresponding leaf spring thicknesses. The leaf spring thickness is taken into account to find the theoretical balancing load.
The analytical stiffness results for the same pre-loads are plotted over the simulated values as dotted lines.
The starting situation for both cases is the same. For the mass, the stiffness is zero at a normalized pre-load of close to 1. For the case of the spring, the stiffness is zero at a pre-load of about 1.8. This value is arbitrary because it depends on the spring length. This spring length is chosen arbitrarily.

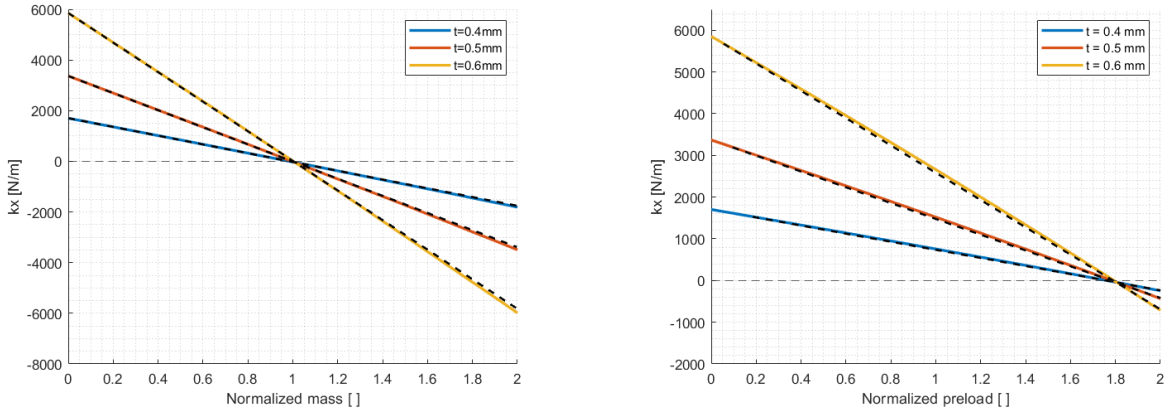

(a) Simulated stiffness in movement direction of the mass (b) Simulated stiffness in movement direction of the spring

Figure 19: Simulated stiffness in movement direction

Support stiffness
The results for the simulated support stiffness can be seen in Figure 20. The support stiffness is plotted over the normalized pre-load, where the pre-load is normalized to the theoretical balancing load for the corresponding leaf spring thicknesses. The simulation was done without and with an initial displacement.
In the case of no initial displacement, the support stiffness is constant over an increasing pre-load. When the system is displaced, it can be seen that the support stiffness decreases with an increasing higher pre-load. Due to the displacement, the initial stiffness is lower compared with the initial stiffness of the undisplaced situation. It can be seen that a thicker leaf spring has a higher support stiffness. The support stiffness decreases more rapidly for larger leaf spring thicknesses.

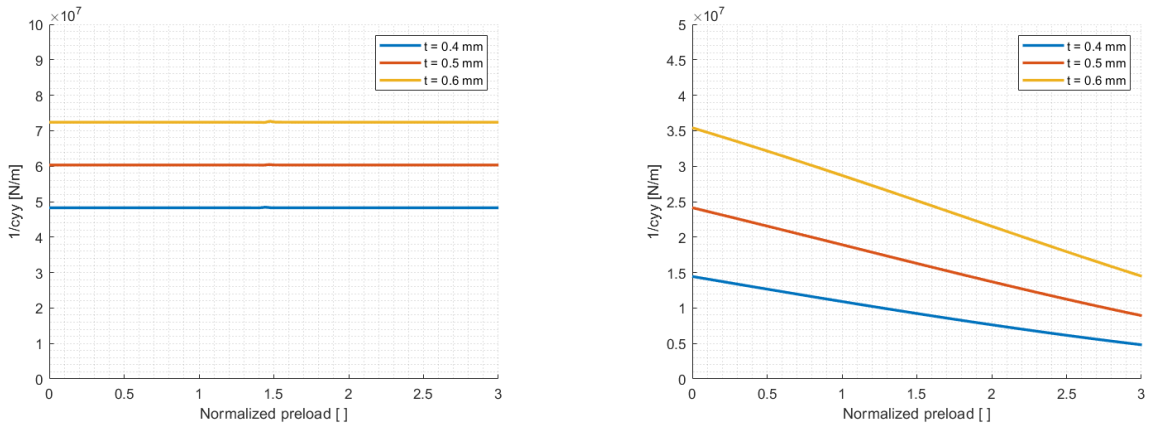

(a) Simulated support stiffness over pre-load, in equilibrium position

(b) Simulated support stiffness over pre-load, with an initial displacement of 5 mm

Figure 20: Simulated support stiffnesses

In Figure 21, the influence of displacement in movement direction on the support stiffness can be seen. In Figure 21a the leaf spring thickness is varied with a constant pre-load of 150N. It can be seen that as the displacement increases, the support stiffness drops. A higher thickness results in a higher support stiffness. The difference between the support stiffness decreases over displacement. In Figure 21b the pre-load is varied with a constant leaf spring thickness of 0.4 mm. It can be seen that the support stiffness drops if the displacement increases. The amount of pre-load has a very small influence on the initial support stiffness. A larger pre-load results in a faster decrease in support stiffness. But overall the pre-load has a smaller effect than the thickness of the leaf spring.

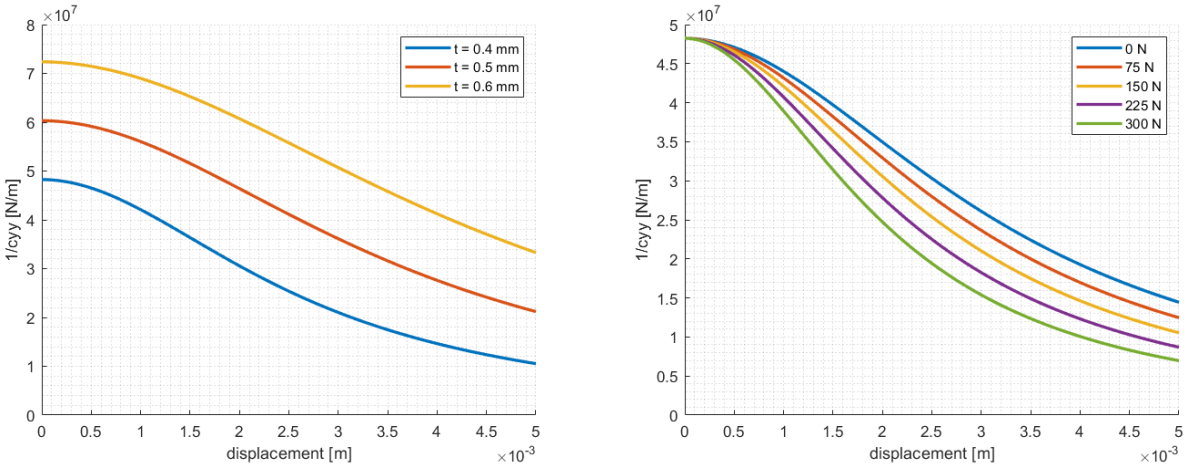

(a) Support stiffness over displacement, with varying leaf spring thicknesses and a pre-load of 150 N

(b) Stiffness in movement direction over displacement, with varying pre-loads and a leaf spring thickness 0.4 mm

Figure 21: Support stiffness over displacement

3.2.2 Maximum stress

The maximum stress per value of normalized pre-load were examined, for both a leaf spring thickness of 0.4 mm, 0.5 mm, and 0.6 mm. This can be seen in Figure 22. The pre-loads were normalized to the theoretical balancing loads for the corresponding thicknesses.

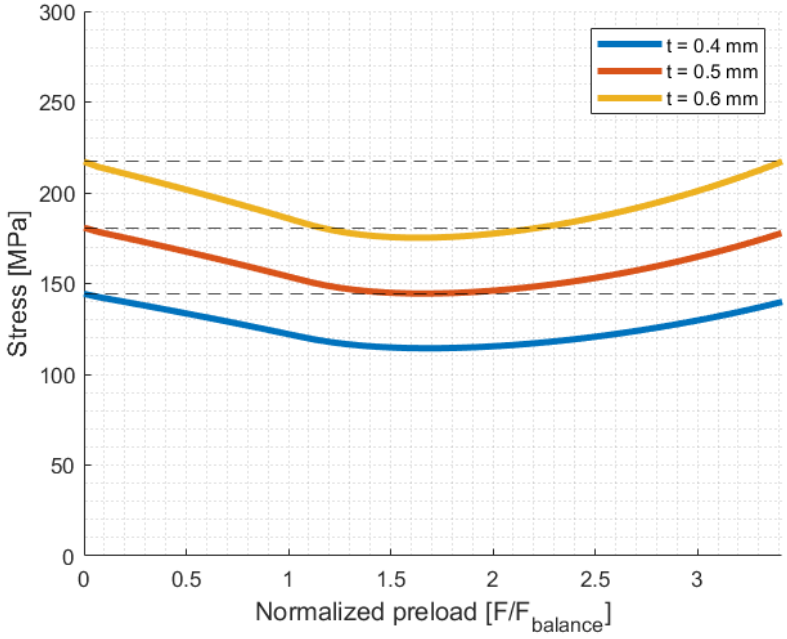

Figure 22: Maximum stress of the system, at deflection

For all the examined leaf spring thicknesses, it can be seen that the maximum stress decreases with a higher pre-load, until a certain point. From that point, the stress stays nearly constant. When the pre-load is further increased, the stress begins to increase again. At a pre-load of 1.5 the theoretical load, the stress is the lowest. The stress begins to increase at a pre-load of approximately 2.1 times the pre-load.
The maximum decrease for leaf springs with a thickness of 0.4 mm was found to be about 29 MPa. For a leaf spring thickness of 0.5 mm, this was found to be around 35 MPa. For a leaf spring thickness of 0.6 mm, it was found to be approximately 40 MPa.

3.3 Modal measurements

Modal measurements can be used to validate the simulations. The eigen frequencies of the simulations and measurements can be compared. The effects of the pre-load and the order of magnitude of frequencies can be examined to validate the simulations.
Modal measurements were done with mass and springs A, B, and C. The results for the mass and spring B can be seen below. The results for springs A and C can be seen in Appendix C. The results are divided into the first eigen frequency, the eigen frequency for the movement direction, and the support frequencies. The measurements were done with a leaf spring thickness of 0.4mm and a leaf spring thickness of 0.5 mm.
No measurement is done for the spring at a force of 0 N, this is because the spring has a zero force, thus adding the spring would have an influence on the eigen frequency. In the case of the mass tests, adding more than 11 kilograms would result in an unbalanced system. The same was the case for the spring at a pre-load of 175 N.

Mode shapes

Below the mode shapes of the simulations and derived with the laser-vibrometer can be seen. In the mode shapes of the laser-vibrometer, the color depicts the amount of movement. Red means a large amount of movement from the equilibrium position. The equilibrium position is defined by the color green. Blue means movement from the equilibrium position, but in the opposite direction that the color red defines. The first mode shape, as can be seen in Figure 23b, is the mode in the movement direction. The second and third modes, as can be seen in Figure 24b and Figure 25b respectively, correspond with the support stiffness of the leaf spring. The mode shapes are very similar but have an opposite movement pattern.
The mode shapes of the laser-vibrometer can be related with the mode shapes from the simulations. It is assumed that the mode shape from the laser-vibrometer in Figure 24 and Figure 25 correspond with the shown mode shapes from the simulations. This is because the eigen frequencies of those modes have almost the same value, both in the simulations and in the measurements.

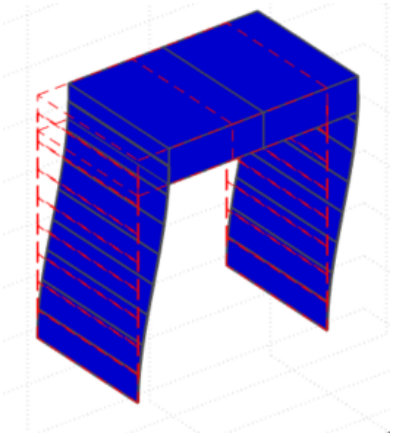

(a) Simulated mode shape corresponding to the first eigen frequency

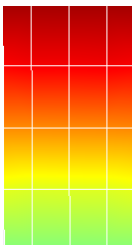

(b) Experimental mode shape corresponding to the first eigen frequency

Figure 23: Mode shape of the first eigen frequency

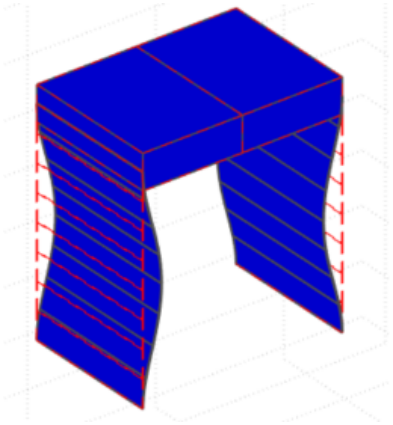

(a) Simulated mode shape corresponding to the second eigen frequency

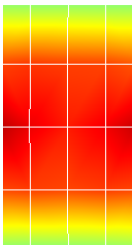

(b) Experimental mode shape corresponding to the second eigen frequency

Figure 24: Mode shape of the second eigen frequency

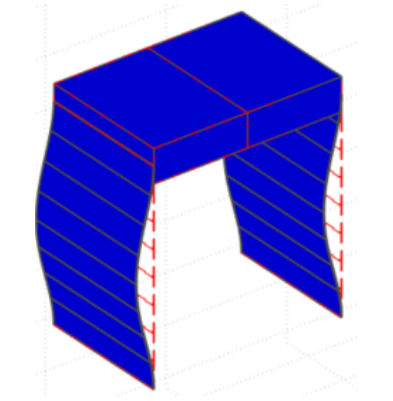

(a) Simulated mode shape corresponding to the third eigen frequency

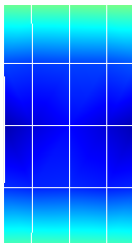

(b) Experimental mode shape corresponding to the third eigen frequency

Figure 25: Mode shape of the third eigen frequency

1st eigen frequency

In Figure 26a and Figure 26b, the results for the mass measurements and the spring measurements can be seen. In the plots, the measured data points are shown. These data points are fitted with a linear regression model. No large outliers in the data points are seen. The simulated data is plotted as a dotted line.

A decrease in eigen frequency can be seen when the pre-load is increased. The decrease is larger in the mass measurements, which is also found in the simulations and the analytical model. This is the case for both leaf spring thicknesses.
The simulations and the measurements match quite well. The measured eigen frequencies are lower than the simulated eigen frequencies. The difference between simulations and measurements is quite constant. This could be due to there being compliance in the system, which is not simulated.
Perfect balance is not achieved. This is due to the fact that the system became unstable before this balance was reached. An unstable system could not be actuated, and thus not measured.
The eigenfrequencies are higher for the larger thickness, this is to be expected, as the stiffness is higher for larger thicknesses. It can be seen that the decrease in eigen frequency of the thicker leaf spring is not as large as the decrease of the thinner leaf springs. This is expected, as the eigen frequency behaves as a square root, thus the decrease becomes larger closer to the balance point. This point is not reached due to spring limitations.

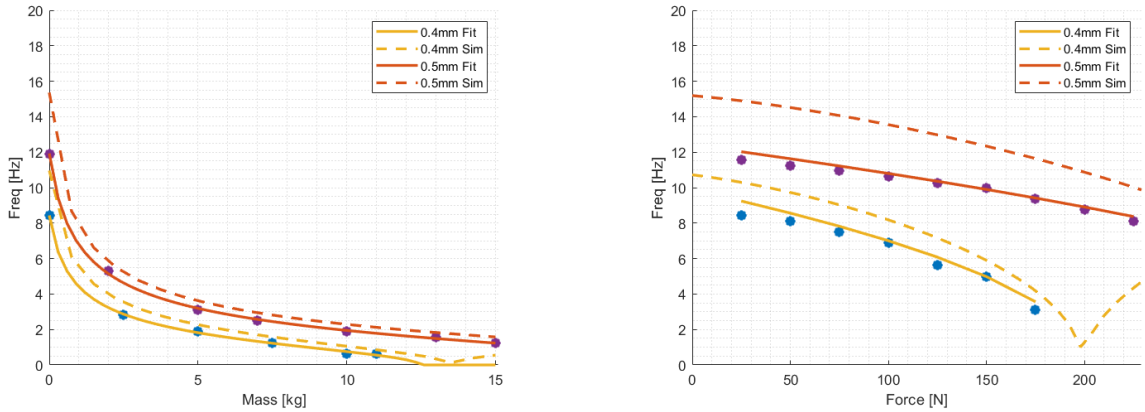

(a) eigen frequency in movement direction, mass and simulated data

(b) eigen frequency in movement direction, Spring and simulated data

Figure 26: eigen frequency in movement direction, simulated and measured data

Support eigen frequencies

In Figure 27a and Figure 28a, the results of the eigen frequency test, in support direction, of the mass can be seen. In Figure 27b and Figure 27b, the results of the eigen frequency tests, in support direction, of the spring can be seen. The data points can be seen, which are fitted with a linear fit. One outlier in data points is seen, the fit gives a good indication of the frequency value at the location of the outlier. The data from the simulations is also shown.
The measured data and the simulated data follow the same trends. The measured eigen frequencies are lower than the simulated values. This difference is constant over the whole range of pre-load. The third eigen frequency is a bit higher than the second one, this also follows from the simulations. A small decrease in support eigen frequencies can be seen for an increasing pre-load.
The eigen frequency of the larger leaf spring thickness is higher compared with the smaller leaf spring thickness. This is expected, as the stiffness increases with increasing leaf spring thickness.

Second eigen frequency

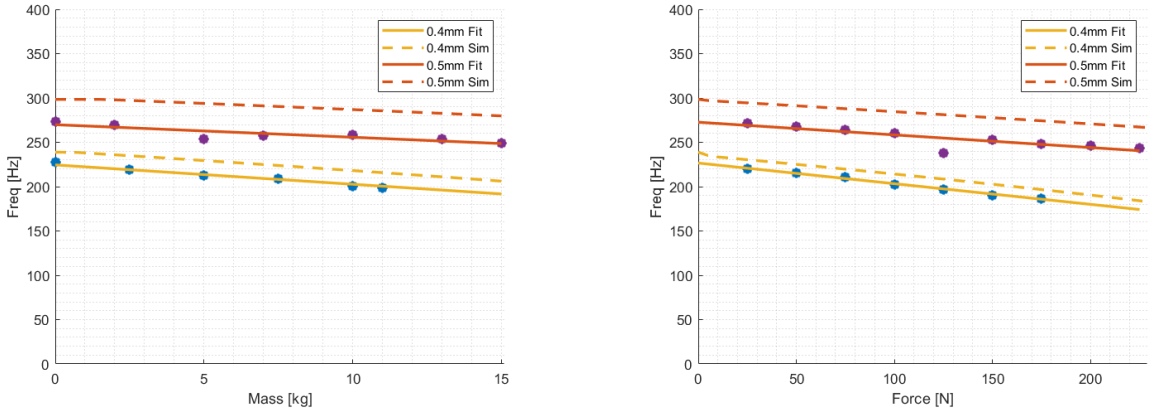

(a) 2nd eigen frequency, mass and simulated data

(b) 2nd eigen frequency, Spring and simulated data

Figure 27: 2nd eigen frequency, simulated and measured data

Third eigen frequency

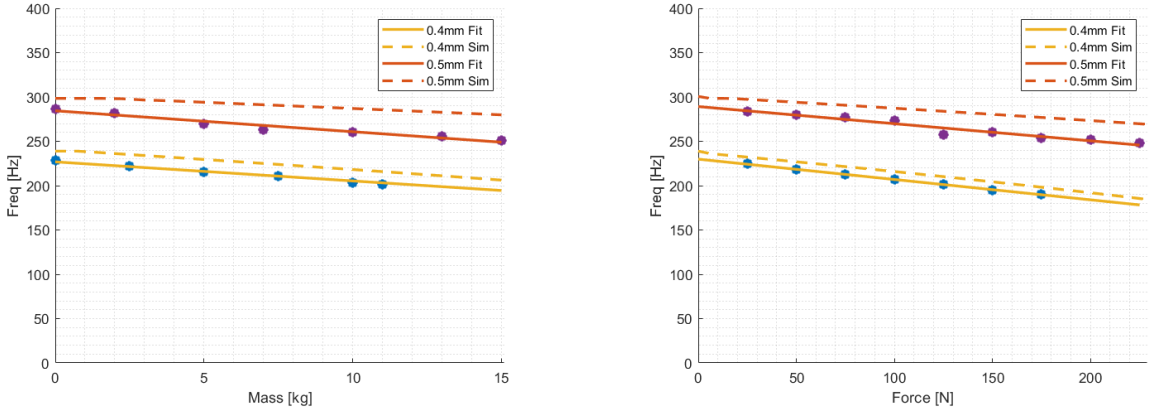

(a) 3rd eigen frequency, mass and simulated data

(b) 3rd eigen frequency, Spring and simulated data

Figure 28: 3rd eigen frequency, simulated and measured data

Comparison with simulations

It can be seen that the eigen frequency simulations and the modal measurements line up quite well. The trend of the eigen frequencies is quite the same. The measured values are a bit lower than the simulated values. This difference is constant over the whole pre-load. This could be unmodelled compliance. This difference is also found in the force-displacement plots. For the first eigen frequency measurement with the spring, the thicker leaf springs do not follow the trend of the simulation as well as the thinner leaf springs. For the thinner leaf springs, the trend is better followed closer to the balance point, it is expected that the same is true for the thicker leaf springs.

Overview of measurements

Below an overview of the measurements and results are given. The start and end values of the used pre-load can be seen in Table 4. In Table 5, the decrease expressed in percentages of the eigen frequencies can be seen. The same decrease is also expressed in Hertz and can be seen in Table 6.

It can be seen that the biggest decrease in eigen frequency in movement direction is achieved with the mass. The system becomes close to being balanced. A reduction of about 60% is achieved for springs B and C. A smaller decrease is achieved for spring A.

The support eigen frequencies also decrease. This decrease is linear, and is not as large when compared with the decrease of the eigen frequencies in movement direction.

Table 4: Used values of pre-load per case

	Start value	End value	Percentage of balancing load
Mass 0.4mm	0 kg	11 kg	79.9%
Mass 0.5mm	0 kg	15 kg	55.8%
Spring A	75N	115N	140.6%
Spring B 0.4mm	25N	150N	129.5%
Spring B 0.5mm	25N	200N	85.3%
Spring C	100N	175N	203.5%

Table 5: Percentage decrease of measured eigen frequencies

	1st eigen frequency decrease	2nd eigen frequency decrease	3rd eigen frequency decrease
Mass 0.4mm	-92.6%	-12.4%	-12.0%
Mass 0.5mm	-89.5%	-9.1%	-12.5%
Spring A	-31.0%	-15.4%	-15.3%
Spring B 0.4mm	-63.0%	-15.2%	-15.3%
Spring B 0.5mm	-29.7%	-10.3%	-12.7%
Spring C	-60%	-23.3%	-23.7%

Table 6: Decrease of measured eigen frequencies expressed in Hertz

	1st eigen frequency decrease	2nd eigen frequency decrease	3rd eigen frequency decrease
Mass 0.4 mm	7.8 Hz	28.1 Hz	27.5 Hz
Mass 0.5 mm	10.6 Hz	25 Hz	35.9 Hz
Spring A	2.8 Hz	33.5 Hz	33.5 Hz
Spring B 0.4mm	5.3 Hz	33.4 Hz	34.4 Hz
Spring B 0.5mm	3.4 Hz	27.8 Hz	35.9 Hz
Spring C	4.7 Hz	48.1 Hz	49.7 Hz

Stiffening effect

It was found from the analytical model and the simulations that the length of springs has an influence on the stiffness in the movement direction, as can be seen in Figure 9. Because the spring length has influence on the stiffness, it also has effect on the eigen frequencies. This can be seen in the modal measurements. Multiple amounts of pre-load can be looked at to see the effect of spring length. Each spring measurement has measurements with a pre-load of 100N, 125N, 150N, and 175N. these measurements can be directly compared with each other.

The eigen frequencies per spring, for 100 N, 125 N, 150 N, and 175 N can be seen in Table 7, Table 8, Table 9 and Table 10. It can be seen that the support eigen frequencies are relatively the same for each spring. It differs with about five Hertz, which results in a percentage difference of about 2.5%.

The eigen frequency in movement direction does differ by a large factor. It can be seen that a longer spring, results in a lower eigen frequency in the movement direction. A difference of 50% can be seen in the case of 175 N.

Table 7: Eigen frequencies comparison at 100 N

Spring	Length	1st eigen frequency	2nd eigen frequency	3rd eigen frequency
A	98 mm	8.75 Hz	203.4 Hz	205.3 Hz
C	129 mm	7.8 Hz	206.6 Hz	210 Hz
B	166 mm	6.9 Hz	202.5 Hz	206.6 Hz

Table 8: Eigen frequencies comparison at 125 N

Spring	Length	1st eigen frequency	2nd eigen frequency	3rd eigen frequency
A	105 mm	8.4 Hz	196.6 Hz	199.1 Hz
C	131 mm	7.2 Hz	200.6 Hz	205.3 Hz
B	180.3 mm	5.6 Hz	196.9 Hz	201.25 Hz

Table 9: Eigen frequencies comparison at 150 N

Spring	Length	1st eigen frequency	2nd eigen frequency	3rd eigen frequency
A	113 mm	7.8 Hz	187.2 Hz	191.9 Hz
C	133 mm	6.6 Hz	190.6 Hz	197.8 Hz
B	194 mm	5 Hz	190.6 Hz	194.7 Hz

Table 10: Eigen frequencies comparison at 175 N

Spring	Length	1st eigen frequency	2nd eigen frequency	3rd eigen frequency
A	120 mm	6.9 Hz	182.8 Hz	185 Hz
C	134.9 mm	5.9 Hz	185.3 Hz	188.1 Hz
B	208.4 mm	3.1 Hz	186.9 Hz	190.6 Hz

4 Discussion

4.1 Measurement limitations

Some limitations were present when doing the experiments, these limitations are discussed below. While these limitations are present, the data gathered can still give relevant information on the behavior of the system. A controller is used to manage the instability in the hysteresis tests. This could not be done at the eigen frequency test, meaning that the maximum force used in the eigen frequency test is lower than the maximum force used in the hysteresis tests.
The limitations are about the force at zero length of the spring and the maximum force that can be reached. There is also a maximum value of mass which can be added. The limitations are mentioned below.

F0
Spring A - F0 is 75N, the shortest length possible of the setup is larger than the minimum length of the spring.
Spring B - F0 is 24.38N.
Spring C - F0 is 85.90N.
Mass - Zero mass can be added

Ending Force
Spring A - Maximum length of spring is reached.
Spring B - Unstable because of large force reached.
Spring C - Unstable because of large force reached.
Mass - Unstable because of the large force reached

VCM Current
There was a limitation on the amount of current the VCM could handle. This was set from -0.5 A to 0.5 A. This was used to determine the possible displacement of the system without pre-load. This displacement was taken as the displacement for the other tests.

4.2 Difference between eigen frequency simulations and modal measurements

In subsection 3.3, a small difference between the simulations and the eigen frequency measurements can be seen. The eigen frequency of the simulations is in general a bit higher than the the measurements. From that, it can be concluded that there is more compliance present in the setup than is modeled in the simulations. This extra compliance could have multiple reasons, which will be discussed below.
This compliance could come from the bolted connections. Bolted connections generally introduce compliance in systems. This was not taken into account in SPACAR.
The initial mass of the setup is measured. This mass is distributed evenly on three top nodes in the simulations. The mass distribution of the setup is different than what is simulated. This could have an effect on the stiffness and compliance of the system.
Miss alignment of components could influence the stiffness of the system. Generally speaking, miss-alignment causes the stiffness in the movement direction to increase and the stiffness in the support direction to stay the same or decrease. As the measured eigen frequencies, in its turn the stiffness, are constantly lower than the simulation, it can be assumed that no large component miss-alignment is present in the system.
Miss alignment can also be present in the form of load miss-alignment. In the simulations, the load was placed in the middle of the top beam. In the setup, the spring is also attached to the middle. It could be the case that the spring hooks apply the force in another than the way it is done in the simulations. In the simulations, the mass is divided over three parts of the top beam. In the experiments, the mass is placed in the middle. This could influence the results.

4.3 Effect of pre-load

The addition of pre-load on the mechanism has effects on the system. The effects will be discussed below.

4.3.1 Effect on eigen frequency and stiffness in movement direction

Eigen frequency in movement direction
The eigen frequency in movement direction decreases as the pre-load on the mechanism increases. This effect was found in the simulations and the eigen frequency measurements, as can be seen in Figure 26. The amount of decrease is dependent on the value of the pre-load, and the method of applying the pre-load. Generally, a higher pre-load causes the eigen frequency to decrease further. At a certain value of pre-load, the eigen

frequency becomes (very close to) zero, at this point the system is balanced. After the balance point is reached, the mechanism is expected to have a zero natural frequency. It can be seen that the eigen frequencies decrease more rapidly for the mass than for the springs, due to the stiffening effect of the springs.

Driving stiffness
The behavior of the eigen frequency can tell something about the corresponding stiffness. An increase in pre-load lowers the stiffness of the leaf spring in the movement direction. The behavior is linear, as can be seen in Figure 19. After a certain value of pre-load is reached, the stiffness becomes zero. At that point the system becomes balanced. Beyond that point, the stiffness becomes negative. The stiffness decreases more rapidly for the mass than for the springs.

4.3.2 Effect on support eigen frequencies and stiffness

Support eigen frequency
The addition of pre-load on the system decreases the support eigen frequencies, as was found in the measurements. This can be seen in Figure 27 and Figure 28. The found decrease was linear. The decrease is approximately the same for the mass and the spring, thus the decrease is not dependent on the method of applying pre-load.

Support stiffness
Applying pre-load does not affect the support stiffness when the system is in an equilibrium position. This can be seen in Figure 20a. When the mechanism is in a deflected position, an increase in pre-load causes the support stiffness to decrease, as can be seen in Figure 20b. The found decrease is linear. The support stiffness does not reach a point where it is (close to) zero.
The support stiffness decreases when the system is displaced, as can be seen in Figure 21. The leaf spring thickness influences the initial value of the support stiffness, but not the behavior over displacement. An increase in pre-load causes the stiffness to drop more rapidly over displacement.

4.3.3 Effect on maximum stress

The addition of pre-load has an effect on the maximum stress present in the leaf springs, as can be seen in Figure 22. The stress decreases with an increasing pre-load, until a certain point where the stress increases again. At a pre-load of about 1.5 times the theoretical balancing load, the maximum stress is the lowest. From there on it increases slowly with an increasing pre-load. At a pre-load of about 2 times the theoretical balancing load, the amount of stress increase increases.
For the leaf spring thickness of 0.4 mm, a decrease of about 22 MPa can be seen at the theoretical balancing force. At about 1.5 times the theoretical balancing force, the maximum stress is the lowest. At that point, the stress decrease is approximately 30 MPa. For the leaf spring thickness of 0.5 mm, a decrease of about 25 MPa is achieved at the theoretical balancing force. At 1.5 times the theoretical balancing force, this decrease is close to 35 MPa. For the leaf spring thickness of 0.6mm, a decrease of approximately 28 MPa was found at the theoretical balancing force. At 1.5 times the theoretical balancing force, a decrease of about 40 MPa was found.

4.4 Influence of pre-load application method

4.4.1 Difference between the addition of mass and springs

The effects of the pre-load differ with the method of implementation. Differences can be seen between the implementation of mass and springs. These differences can be examined in the eigen frequency test and the hysteresis tests.

Eigen frequencies
It was found that a lower pre-load is required to reach the balance point for the mass when compared with the springs. This can be seen in Figure 19 and Figure 26. This is due to the fact that the spring has a force component opposite of the movement direction.
The support eigen frequencies of the mass and the springs have approximately the same value, as can be seen in Figure 27 and Figure 28. The decrease of the support eigen frequencies is approximately the same for both the mass and the springs.

Hysteresis
The first part of the hysteresis curves for the mass and spring cases look very similar, as can be seen in Figure 14, 15 and 16. An increase of pre-load results in a flatter laying line, thus a lower actuation stiffness. A lower amount of pre-load is needed to reach the balancing point for the case of the mass. This is also found in the eigen frequency tests. A slightly larger current hysteresis has been found in the case of the mass measurements. No large conceivable difference has been seen in the displacement hysteresis. This can be seen in Figure 17. So no large difference in hysteresis is seen between the attachment methods.

Largest difference
The largest difference found between the springs and the mass is the larger decrease of the eigen frequency in movement direction for the mass. This is due to the stiffening effect of the spring. No large difference can be seen between the hysteresis of the system and the support frequencies.

4.4.2 Stiffening effect of the spring

A stiffening effect is present when the pre-load is applied with springs. This has been found in the analytical model. From Figure 6 and Figure 8, it follows that more pre-load is needed to balance the system in case of the spring. It was also found that the spring length has an influence on the amount of extra pre-load needed. This can be seen in section 3.3, Figure 9 and Figure 10.
Multiple modal measurements were done with different spring lengths. The eigen frequencies at the same pre-loads and different lengths are examined. These eigen frequencies can be seen in Table 7, Table 8, Table 9 and Table 10. It can be seen that the spring length has an effect on the first eigen frequency. The spring length has almost no influence on the support eigen frequencies of the system.
When a longer spring is attached, the component of the force in the movement direction decreases, meaning more of the pre-load is applied in the intended direction. This effect can be seen in the tables mentioned above. For a pre-load of 100 N, the difference in eigen frequency is smaller than for a higher amount of pre-load. A difference of about 25% in eigen frequency can be seen in the case of a pre-load of 100 N. This is with a length difference of about 70%. In the case of a larger pre-load, a difference of 50 % in eigen frequency can be seen in the first eigen frequency for a length difference of about 100 %.
To overcome this stiffening effect, more pre-load needs to be applied, as can be seen in Figure 9. The amount of extra pre-load needed decreases as the spring length increases. To achieve a relatively good balance for a relatively low amount of pre-load, a long spring is required. A higher pre-load is needed to balance with a short spring when compared with a longer spring. A higher pre-load results in a decrease in support stiffness and has an influence on the maximum stress in the leaf springs. An increase in pre-load also results in a larger value of the pre-load opposite of movement direction, to overcome this extra stiffening effect, an increase in pre-load is needed.

4.5 Point of static balance

The point of static balance had been found in multiple ways. The theoretical balance point can be calculated with the buckling equation, as can be seen in Equation 1. The analytical force displacement curves can be used to determine the balance point. With the simulations, the balance can be found with the force displacement plots and the stiffness analysis. The balance point was found with the hysteresis measurements, and can be estimated with the modal measurements. These found balances forces can be seen in Table 11. The balance point of the force displacement of the spring is found with Figure 35. It can be seen that the balance points of the mass lay below the simulated and theoretical values. For the spring the values are higher than the mass, as is expected.

Table 11: Found balancing forces, for leaf spring thickness of 0.4mm

	Mass [kg]	Spring (clamped) [N]	Spring (hanging) [N]
Theoretical	13.8	135	135
Force displacement	13.5	203	203
Hysteresis measurements	11.75	198	193
Modal measurements	12.25	≈ 200	≈ 200

4.6 Theoretical support stiffness increase

The leaf springs can only experience a certain amount of stress before yielding. As can be seen in Figure 22, the stress of the leaf spring increases with increasing leaf spring thickness. This means that only up to a certain leaf spring thickness is viable for this mechanism. What also can be seen in Figure 22, is that the stress decreases

as the pre-load increases, up to a certain point. This stress decrease could be used to (partially) negate the stress increase of an increasing leaf spring thickness. It can be seen that at a pre-load of about 1.5 to about 2.2 times the theoretical balancing load, the maximum stress is equal to the stress in the mechanism with a lower leaf spring thickness and no pre-load applied. This means that at a pre-load of 1.5 times the balancing load, the leaf spring thickness can increase by 0.1 mm.
In Figure 20a, it can be seen that a thickness increase of 0.1 mm leads to a support stiffness increases by $1.2 \cdot 10^7 N/m$ when in equilibrium position. This is an increase of about 25%. When deflected the support stiffness increases by approximately $0.8 \cdot 10^7 N/m$, as can be seen in Figure 20b. This is an increase of about 80%.
An increase in leaf spring thickness also results in an increase in actuation stiffness. This can be seen in Equation 2 and Figure 19. From the equation, it follows that the thickness increase has an influence with the power of three on the initial actuation stiffness. This increase in actuation stiffness can be negated by applying a pre-load. For the case of the mass, the system is balanced at 1.5 times the theoretical balancing load. For the spring it depends on the spring length. From Figure 9, it follows that the spring length needs to be around 2.2 the leaf spring length, for a pre-load of 1.5 times the balancing load.

4.7 Optimum spring and system properties

Multiple optimums can be found for the system properties, dependent on the desired behavior. In Table 12 different system properties can be seen for different leaf spring thicknesses and different amounts of pre-load. The behavior is examined for the theoretical balancing load, 1.5 and 2 times the theoretical balancing load.

Table 12: System properties for certain values of leaf spring thickness and pre-load, evaluated at a deflection of 5 mm and spring length of 2.5 L_f.

	t [mm]	kxx [N/m]	kyy [N/m]	Stress [MPa]	Pre-load [N]	Optimal spring length $[L_s/L_f]$ eq. 30
Zero pre-load	0.4	1702	$1.44 \cdot 10^7$	144.2	0	-
Balancing load	0.4	532	$1.09 \cdot 10^7$	122.6	135.1	≈ 10
1.5 balancing load	0.4	-71	$0.92 \cdot 10^7$	114.7	202.7	2.45
2 balancing load	0.4	-621	$0.76 \cdot 10^7$	115.0	270.2	1.6
Zero pre-load	0.5	3367	$2.41 \cdot 10^7$	180.6	0	-
Balancing load	0.5	1115	$1.88 \cdot 10^7$	156.6	263.9	≈ 10
1.5 balancing load	0.5	-97	$1.62 \cdot 10^7$	145.8	395.8	2.45
2 balancing load	0.5	-1281	$1.36 \cdot 10^7$	145.4	527.8	1.6
Zero pre-load	0.6	5851	$3.54 \cdot 10^7$	216.97	0	-
Balancing load	0.6	1889	$2.88 \cdot 10^7$	188.2	456	≈ 10
1.5 balancing load	0.6	-142	$2.53 \cdot 10^7$	176.1	684	2.45
2 balancing load	0.6	-2205	$2.15 \cdot 10^7$	176.6	912	1.6

It can be seen that the system properties differ for different values of pre-load and different leaf spring thicknesses. The optimum configuration depends on which behavior is desired.
For a low actuation stiffness, a pre-load of 1.5 times the balancing load or higher is desired. Thinner leaf springs also result in lower actuation stiffness. For a high support stiffness, thick leaf springs with a low pre-load are desired. For low maximum stress, the best range of pre-load is between 1.5 and 2 times the theoretical balancing load, thinner leaf springs also result in lower stress.

4.8 Difference in hysteresis for different spring attachment methods

In Figure 15 and Figure 16 the hysteresis curves for the clamped spring and the hanging spring can be seen. In the case of the hanging spring, the spring is able to rotate around the screw.
The same trend of driving stiffness decrease at a higher pre-load can be seen for both cases. For the same amount of pre-load, the same amount of needed force is seen. The amount of quantified current hysteresis does not differ between both cases.
There is a difference in displacement hysteresis, as can be seen in Figure 17b. This difference is due to the fact that the hysteresis curves of the clamped spring are laying more flat than the hysteresis curves taken for the hanging spring. In the hysteresis curves, it can be seen that the hysteresis behavior is very similar.
The amount of needed pre-load to reach the balance point differs between both cases. The difference is about 5 N. This difference could be caused by the starting position of the spring. The starting position is chosen on the minimum length the spring can reach, the attachment method could influence this starting position. A higher or lower starting position could influence the amount the spring has to move to reach the balancing point. This

could the balancing force to differ.

From this, it can be concluded that there is no significant difference between the spring attachment methods in these experiments. In this case, a small deflection was reached in the measurements, a larger deflection could show an increase in hysteresis.

5 Conclusion

The first eigen frequency decreases with an increasing pre-load. The same trend can be seen in the measurements as in the analytical model and the simulations. The support eigen frequencies decrease a bit with an increasing pre-load. This can also be seen in the simulations. The measured frequencies are a bit lower than the simulated values, this difference is constant over the range of pre-load. From this, the simulations and analytical model can be validated.

From the hysteresis measurements, the amount of pre-load to balance the mechanism was found. For the mass, the system became balanced at a pre-load of 11.75 kg. For the clamped spring, the system became balanced for a pre-load of about 198 N. The system with the hanging spring became balanced at a pre-load of 193 N. Increasing the pre-load beyond these points results in negative stiffness behavior.

The maximum stress reduces with an increasing pre-load till a certain value. The maximum stress decrease was found to be at 1.5 times the theoretical balancing load. The maximum decrease for leaf springs with a thickness of 0.4 mm was found to be about 29 MPa. For a leaf spring thickness of 0.5 mm, this was found to be around 35 MPa. For a leaf spring thickness of 0.6 mm, it was found to be approximately 40 MPa.
The support stiffness increases with increasing leaf spring thickness. The stress also increases with increasing leaf spring thickness. The maximum stress decrease from an applied pre-load can negate this effect and make it possible to increase the leaf spring thickness. An increase of 0.1 mm in thickness results in a stiffness increase of about 25% when in an equilibrium position. When the deflected, the support stiffness increases with about 80%.

Applying pre-load with springs results in a stiffening effect of the spring. Part of the spring force is in the opposite direction of the movement direction. A longer spring results smaller amount of said stiffening effect. At one time the theoretical balancing load, the spring length needs to be approximately ten times the length of the leaf spring to negate this effect. At two times the theoretical balancing load, the spring length needs to be around 1.6 times the length of the leaf spring.

No large difference in hysteresis can be seen between the different spring attachment methods. The same displacement is reached for the same applied current. The behavior under pre-load is approximately the same. The hanging spring needs a bit less pre-load to reach the balancing point. No large difference in terms of hysteresis was found between the springs and the mass.

6 Recommendations

Further steps could be taken to improve the research and gather more information on applying pre-load and its effects. These steps are discussed below.

Increased amount of data points
In this research eigenfrequency tests were done. For each amount of pre-load, one measurement was done. This gave usable and valid results, but an increase in data points could increase the accuracy of the results. The same is the case for the hysteresis measurements. The current- and displacement hysteresis could become more accurate if more data points are present.
It could also be beneficial if an eigen frequency test could be done where the pre-load is increased to the balance point and further than the balance point. This was not possible with the current setup. If it is possible, the balance point could be determined more exactly and the behavior beyond the balance point could be analysed.

Comparison between clamped and hanging spring
In this research, a comparison is made between the hysteresis of a spring hanging on a screw and a clamped spring. Because this is done with only one spring, there is a small sample size. It could be beneficial to increase this sample size, such that a better conclusion can be gotten on the effects of the way the spring is attached.
The measurements were done with a small deflection, a larger deflection of the mechanism could show a noticeable difference between the methods of attaching the spring.
The starting position of the spring was chosen by hand, a method of being able to find the starting point could be beneficial.

Stress verification
A decrease in stress was found in the simulations. This decrease was not verified by the test, as the eigenfrequencies were. It could be assumed that the stresses in the simulations are correct, but a stress verification test could be beneficial. That way the validity of the results could be shown.
A possibility for this would be by adding strain gauges on the leaf spring, near the clamps, and in the middle. This could give a good indication of the values of the stress and the stress distribution.

Examining other flexure-based mechanisms
In this research, a parallel leaf spring mechanism was examined. A parallel leaf spring mechanism is one of many flexure-based mechanisms. Implementing pre-load on other flexure-based mechanisms and examining the behavior of those systems could give relevant information on a general way of implementing pre-load, and the effects of the implemented pre-load.

Guideline for applying pre-load
A guideline can be made for implementing pre-load in mechanisms. Multiple methods could be introduced and the advantages and disadvantages of for example adding mass and/or springs could be given. The optimum settings and system properties could be given for multiple cases, for example low actuation stiffness or high support stiffness.

References

[1] L. Howell, *Compliant Mechanisms*. A Wiley-Interscience publication, Wiley, 2001.

[2] K. Hoetmer, J. Herder, and C. Kim, "A building block approach for the design of statically balanced compliant mechanisms," 01 2009.

[3] J. Gallego Sanchez and J. Herder, "Criteria for the static balancing of compliant mechanisms," vol. 2, 01 2010.

[4] N. Tolou, J. Gallego Sanchez, and J. Herder, "Statically-balanced compliant micromechanisms," *Mikroniek*, vol. 50, pp. 20–25, 01 2010.

[5] J. Herder, *Energy-free Systems; Theory, conception and design of statically balanced spring mechanisms*. PhD thesis, 11 2001.

[6] T. L. Thomas, V. Kalpathy Venkiteswaran, G. K. Ananthasuresh, and S. Misra, "Surgical Applications of Compliant Mechanisms: A Review," *Journal of Mechanisms and Robotics*, vol. 13, 01 2021. 020801.

[7] E. G. Merriam and L. L. Howell, "Non-dimensional approach for static balancing of rotational flexures," *Mechanism and Machine Theory*, vol. 84, pp. 90–98, 2015.

[8] S. Henein, "Short communication: Flexure delicacies," *Mechanical Sciences*, vol. 3, 01 2012.

[9] E. Merriam, M. Colton, S. Magleby, and L. Howell, "The design of a fully compliant statically balanced mechanism," vol. 6, 08 2013.

[10] H. Liang, G. Hao, O. Z. Olszewski, and V. Pakrashi, "Ultra-low wide bandwidth vibrational energy harvesting using a statically balanced compliant mechanism," *International Journal of Mechanical Sciences*, vol. 219, p. 107130, 2022.

[11] J. van Eijk and J. Dijksman, "Plate spring mechanism with constant negative stiffness," *Mechanism and Machine Theory*, vol. 14, no. 1, pp. 1–9, 1979.

[12] J. de Jong, S. Theans, L. Epping, and D. Brouwer, "Improving support stiffness of flexure mechanisms by statically balancing," pp. 45–48, nov 2021. Publisher Copyright: © 2021 Proceedings - 36th ASPE Annual Meeting. All rights reserved.; 36th Annual Meeting of the American Society for Precision Engineering, ASPE 2021 ; Conference date: 01-11-2021 Through 05-11-2021.

[13] K. Hoetmer, G. Woo, C. Kim, and J. Herder, "Negative stiffness building blocks for statically balanced compliant mechanisms: Design and testing," *Journal of Mechanisms and Robotics*, vol. 2, p. 041007, 11 2010.

[14] JPE, "Precision point." https://www.jpe-innovations.com/precision-point/beam-theory-buckling/. Beam theory: buckling.

[15] J. B. Jonker and J. P. Meijaard, *SPACAR — Computer Program for Dynamic Analysis of Flexible Spatial Mechanisms and Manipulators*, pp. 123–143. Berlin, Heidelberg: Springer Berlin Heidelberg, 1990.

[16] Akribis systems, *AVM series*.

[17] RLS, *RLS-RLB*.

[18] "Tevema." https://www.tevema.com/. Accessed: 2023-04-10.

[19] X. Feng, Z. Duan, Y. Fu, A. Sun, and D. Zhang, "The technology and application of voice coil actuator," in *2011 Second International Conference on Mechanic Automation and Control Engineering*, pp. 892–895, 2011.

[20] R. Aarts and J. van Dijk, *Dictaat Inleiding Systeem- en Regeltechniek (Lecture notes 113117, 113115, 280214)*. Werktuigbouwkundige automatisering / Mechanical Automation (MA), 2008.

[21] "Psv-500 scanning vibrometer." https://www.polytec.com/int/vibrometry/products/full-field-vibrometers/psv-500-scanning-vibrometer. Accessed: 2023-07-3.

A Spring identification

An identification has been done on the springs to determine the stiffnesses. This was done to see if the springs are up to manufacturer specs and to better calculate the needed spring length for the measurements. The results can be seen in Figure 29a, 29b, and 30a. Because the largest spring has a higher F_0, the spring did not displace for the first measurement points. A zoomed-in version of the linear behavior is made and can be seen in Figure 30b. The results of the stiffnesses are summarized in Table 13. It can be seen that the springs with the lower stiffness match the manufacturer specified stiffnesses quite well. The measured stiffness of the large spring with high stiffness differs more from the specified stiffness. This could be due to there being fewer data points, thus a measurement error having a larger effect on the total.

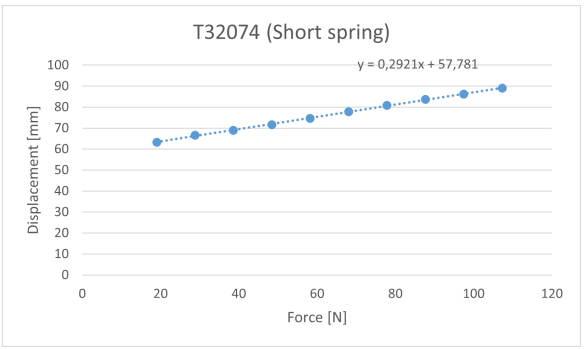

(a) Force displacement plot of the smallest spring

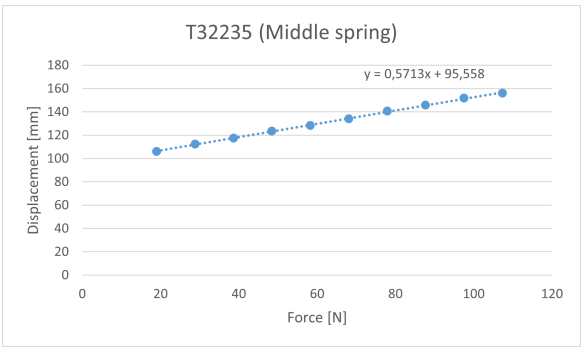

(b) Force displacement plot of the middle spring

Figure 29: Force displacements plots used to derive the spring stiffness of the smallest and middle spring

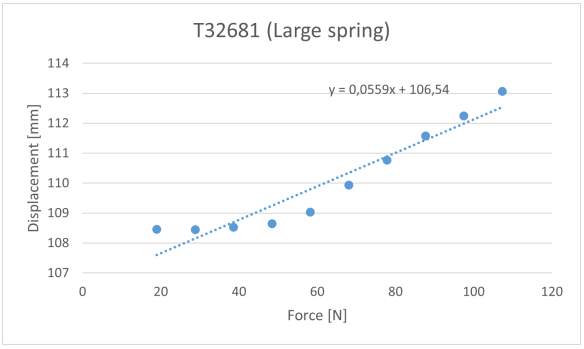

(a) Force displacement plot of the largest spring

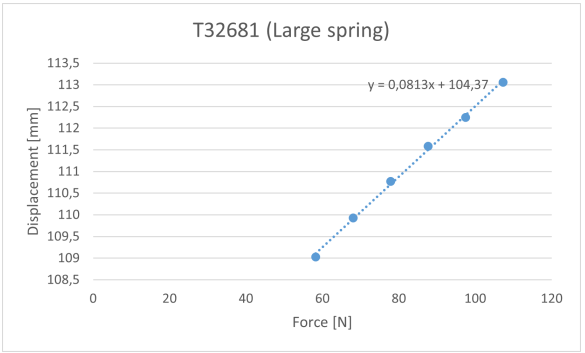

(b) Zoomed-in on the linearly increasing part of the force-displacement plot of the largest spring

Figure 30: Force displacement plot and zoomed-in version used to derive the spring stiffness of the largest spring

Table 13: Measured spring stiffnesses compared with the specified stiffnesses

	Report name	Name	Measured stiffness [N/mm]	Specified stiffness [N/mm]	Difference	L_0 [mm]
Short	A	T32074	3.423	3.33	3%	75.8
Middle	B	T32235	1.750	1.71	2%	123
Large	C	T32681	12.3001	11.34	8%	128

B Mass equivalent for the used controller

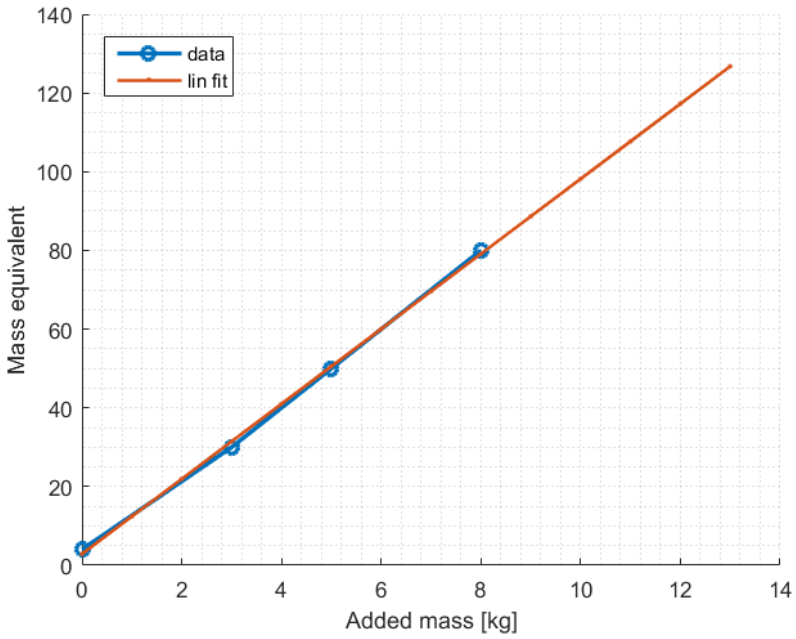

Figure 31: Measured and fitted mass equivalents

C Eigenfrequency measurements spring A and C

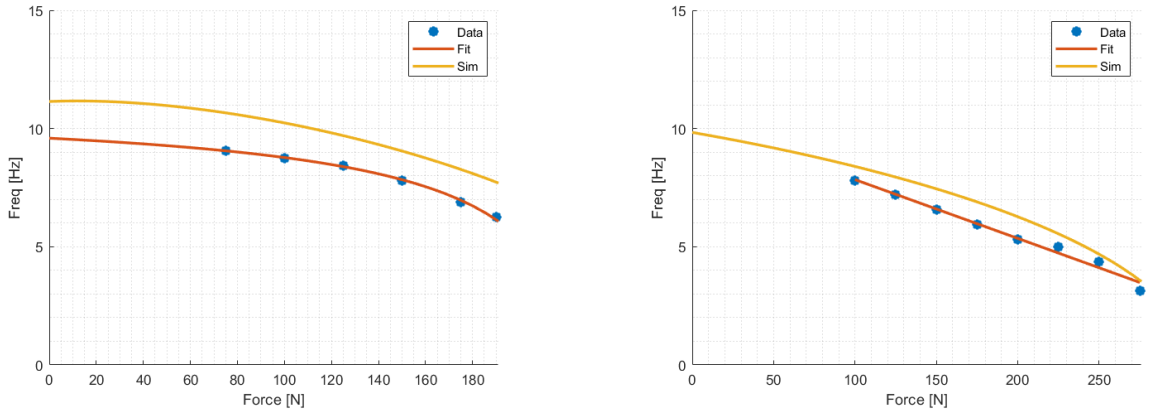

(a) Eigenfrequency in movement direction, Spring A and simulated data

(b) Eigenfrequency in movement direction, Spring C and simulated data

Figure 32: Eigenfrequency in the movement direction, simulated and measured data

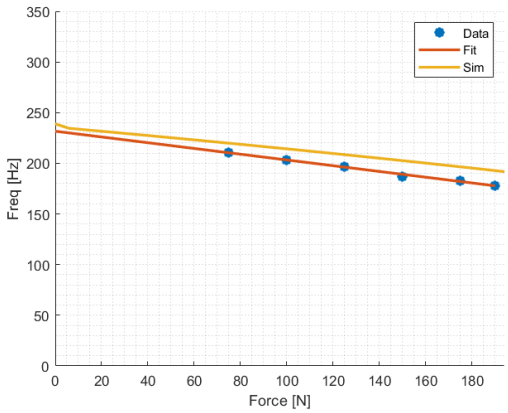

(a) 2nd Eigenfrequency, Spring A and simulated data

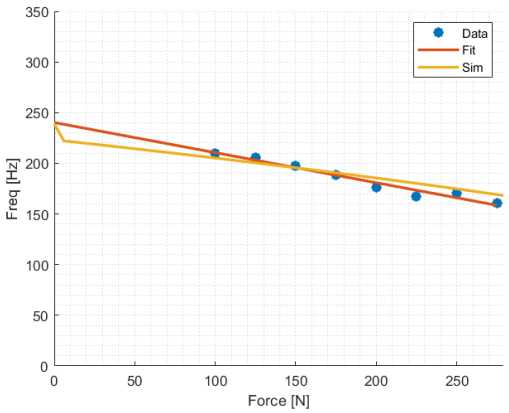

(b) 2nd Eigenfrequency, Spring C and simulated data

Figure 33: 2nd Eigenfrequency, simulated and measured data

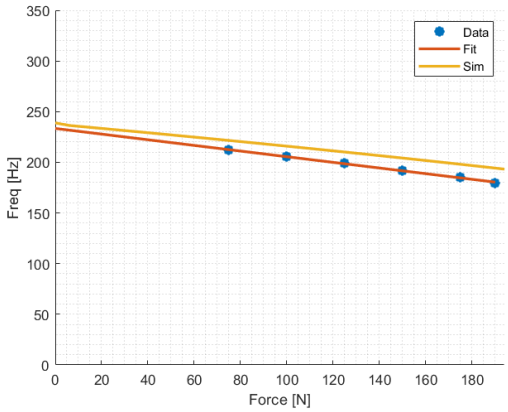

(a) 3rd Eigenfrequency, Spring A and simulated data

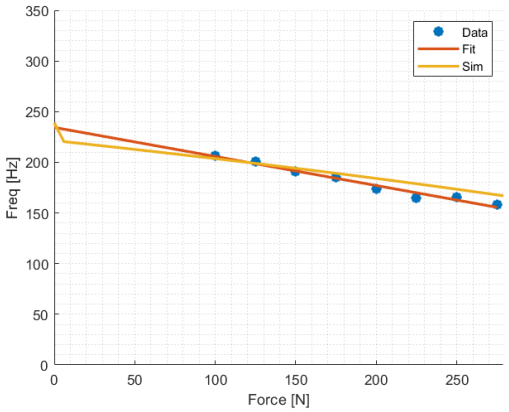

(b) 3rd Eigenfrequency, Spring C and simulated data

Figure 34: 3rd Eigenfrequency, simulated and measured data

D Actuation stiffness of spring corresponding with measurement

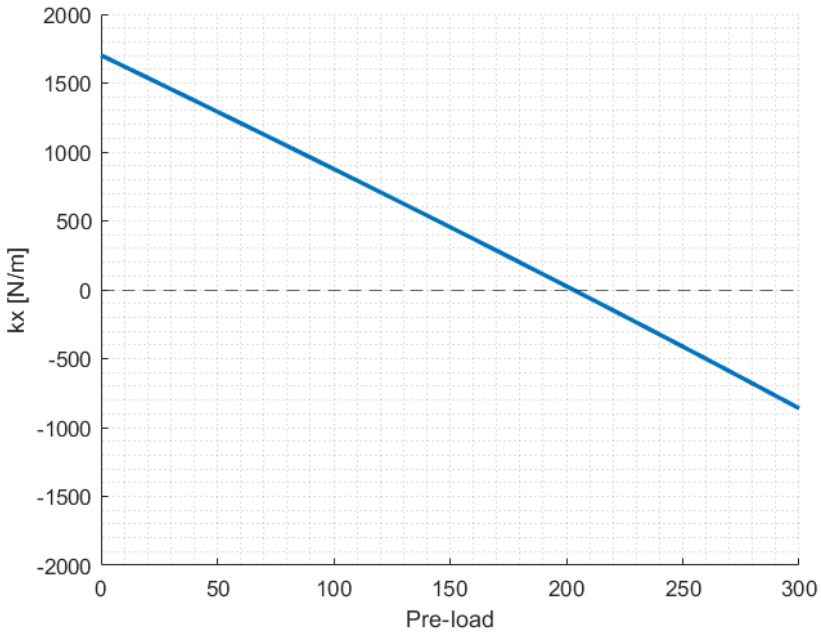

Figure 35: Actuation stiffness for spring length corresponding with measurements with a pre-load of 200 N